Flood Hazard Mapping Using Integrated Multi-Parametric AHP-GIS and SFFM: Case Study On Adama City

Kemal Jambo Boru

A thesis Submitted to the department of Water Resources Engineering

School of Civil Engineering and Architecture

Presented in partial fulfillment of the requirement for the degree of Master's in Water Resources Engineering (in Hydraulic Engineering)

Office of Graduate Studies

Adama Science and Technology University

October, 2023

Adama, Ethiopia

Flood Hazard Mapping Using Integrated Multi-Parametric AHP-GIS and SFFM: Case Study On Adama City

Kemal Jambo Boru

Advisor: Dereje Birhanu (PhD)

A thesis Submitted to the department of water resources engineering
School of civil engineering and architecture

Presented in partial fulfillment of the requirement for the degree of Master's in Water Resources Engineering (in Hydraulic Engineering)

Office of Graduate Studies
Adama Science and Technology University

October, 2023

Adama, Ethiopia

DECLARATION

I hereby declare that this Master Thesis entitled "Flood Hazard Mapping Using Integrated Multi-Parametric AHP-GIS and SFFM: Case Study On Adama City" is my original work. That is, it has not been submitted for the award of any academic degree, diploma or certificate in any other university. All sources of materials that are used for this thesis have been duly acknowledged through citation

Name of student	Signature	Date

RECCOMENDATION OF ADVISORS

I, the major advisor of this thesis, hereby certify that I have read the revised version of the thesis entitled "Flood Hazard Mapping Using Integrated Multi-Parametric AHP-GIS and SFFM, Case Study On Adama City" is prepared under my guidance by Kemal Jambo. submitted in partial fulfillment of the requirements for the degree of Mater's of Science in Water Resources Engineering specialization in (Hydraulic Engineering). Therefore, I recommend the submission of revised version of the thesis to the department following the applicable procedures.

Major Advisor/Supervisor	Signature	Date
Co-advisor/Co-supervisor	Signature	Date

APPROVAL SHEET

I, the advisor of the thesis entitled "Flood hazard mapping using integrated multi-parametric AHP-GIS and SFFM: Case Study on Adama City" and developed by Kemal Jambo, hereby certify that the recommendation and suggestions made by the board of examiners are appropriately incorporated into the final version of the thesis.

______________________	______________	___________
Major Advisor	Signature	Date
______________________	______________	___________
Co-advisor	Signature	Date

We, the undersigned, members of the Board of Examiners of the thesis by Kemal Jambo have read and evaluated the thesis entitled "Flood hazard mapping using integrated multi-parametric AHP-GIS and SFFM: Case Study on Adama City" and examined the candidate during open defense. This is, therefore, to certify that the thesis is accepted for partial fulfillment of the requirement of the degree of Master of Science in Hydraulic Engineering.

______________________	______________	___________
Chairperson	Signature	Date
______________________	______________	___________
Internal examiner	Signature	Date
______________________	______________	___________
External examiner	Signature	Date

Final approval and acceptance of the thesis is contingent upon submission of its final copy to the Office of Postgraduate Studies (OPGS) through the Department Graduate Council (DGC) and School Graduate Committee (SGC).

______________________	______________	___________
Department Head	Signature	Date
______________________	______________	___________
School Dean	Signature	Date
______________________	______________	___________
Office of post graduate studies, Dean	Signature	Date

ACKNOWLEDGEMENTS

I am deeply grateful to my advisor, Dereje Birhanu (Ph.D.), whose guidance, expertise, and unwavering support have been invaluable throughout my thesis journey. I extend my sincere appreciation to the Adama City Meteorological Agency and the Adama City Municipality for generously providing the essential data that formed the backbone of my research.

I am sincerely grateful to Oda Bultum University for providing me with the remarkable opportunity to pursue my M.Sc. degree and for generously offering full sponsorship, for which I am truly thankful.

My fellow researchers and colleagues have been constant sources of inspiration and collaboration, for which I am thankful. I also extend my heartfelt thanks to the dedicated staff of the ASTU Water Resources Department and all those who extended their helping hands; each contribution has left an indelible mark on my work.

My deepest gratitude goes to my family, whose unwavering support, encouragement, and understanding have sustained me throughout this journey. Your belief in my abilities has been a driving force, and I am profoundly appreciative for the sacrifices you've made to facilitate my academic pursuits.

Additionally, I extend my appreciation to every individual who played a role, no matter how small, in helping me navigate the challenges and complexities of this research. In conclusion, this accomplishment would not have been possible without the collective effort, encouragement, and assistance of the aforementioned individuals and institutions.

TABLE OF CONTENTS

CONTENTS PAGES

LIST OF TABLES

LIST OF FIGURES

LIST OF ACRONYM AND ABBREVIATIONS

AHP	Analytical Hierarchy Process
CI	Consistency Index
CHIRPS	Climate Hazards Group InfraRed Precipitation with Station data
CR	Consistence Ratio
DD	Drainage Density
DEM	Digital Elevation Model
ERA	Ethiopian Road Authority
FAO	Food and Agricultural Organization
FRI	Flood Risk Index
GEV	Generalized Extreme Value
GIS	Geographical Information System
HEC-SSP	Hydrologic Engineering Center - Statistical Software Package
IMD	Indian Meteorological Department
IDF	Intensity Duration Frequency
LC	Linear Combination
LTS	Linear Transformation Scale
LULC	Land Use Land Cover
FRI	Flood Risk Index
MCDA	Multi Criterion Decision Analysis
MCE	Multi Criterion Evaluation
PCP	Precipitation
RF	Rainfall
RFI	Rainfall Intensity
RIW	Relative Importance Weight
SFFM	Super-Fast Flood Model
WMO	World Meteorological Organization

ABSTRACT

Flooding is one of the most common natural disasters, often with disastrous consequences, affecting 170 million people worldwide each year. East Africa has been facing flooding problems due to heavy rainfall. Around 2.5 million people, just in Ethiopia, Sudan, and South Sudan, have been defenseless against the flood water. At least 1.3 million people have been affected by flooding; 481,000 have been relocated; and 360 individuals have lost their lives as a result of devastating floods in the region. Adama City has experienced flooding problems that have led to the displacement of communities in some areas of the sub-city, destroyed different infrastructures, washed away houses, and affected people and the city's economy. The main focus of the study was mapping the flood hazard and computing flood inundation depth in Adama City using integrated multi-parametric Analytical Hierarchy Process (AHP) with Geographical Information System (GIS) and the Super-Fast Flood Model. To achieve these objectives, the AHP-GIS model was employed with the methodology of collecting hydrological, meteorological, and geophysical data. Furthermore, residents and different experts were interviewed to make judgments among flood causative factors and validate the model's results. Eight flood causative factors such as rainfall, slope, elevation, land use land cover, road network, drainage density, storm drains, and soil type were utilized to generate a flood hazard map of the City. The super-fast flood model simulated flood inundation depth for three cases, such as the past flood event of April 18, 2000, rainfall intensity (35.5 mm/hr) and rainfall intensity of both Indian Meteorological Department (IMD) 55.6 mm/hr and Ethiopian Road Authority (ERA) 78 mm/hr of the 50-year return period for a 0.5-hour storm duration. The generated flood hazard map indicated that Irrecaha, Migira, and some parts of Gara Lugo Kebeles were at high risk of flooding. For past flood event simulations, flood depth was in the range of 0 to 1.8 meters. A 0–1.95 meter and 0–2.3 meter flood inundation depths were obtained from 50-year simulation scenarios of the IMD and ERA methods of Rainfall Intensity (RFI), respectively. The result inferred that the maximum flood depth appeared in Irrecha and Migira kebeles. The obtained model outputs were validated based on experts and local resident's interviews, as there was no single stream flow gauge station in the city and limited satellite products capturing water extent during rainfall events. The results of the study revealed that poor drainage networks in very low-elevation areas aggravated the flood hazard in the city. This study will be helpful in flood protection, planning and construction of any projects along the city's flood hazard area, and planning effective emergency responses for flood hazard areas in the city. Furthermore, the developed IDF curve will be helpful in planning and designing the drainage system of the city.

Keywords: *Vulnerability, flood hazard map, AHP-GIS, IMD, ERA, Super-fast flood model*

1. INTRODUCTION

1.1. Background

Flooding is a natural hazard that affects human life and the ecosystem globally, causing catastrophic disasters. Most flood-induced socioeconomic losses are exacerbated by unabated urban development, population upsurges, unregulated municipal systems, and indiscriminate land use (Hategekimana et al., 2018). Climate change and an increase in human-induced land-use changes make flooding more severe and frequent, which puts pressure on river channels and alters the river morphology (Hagos et al., 2022). Flooding is one of the most common natural disasters, often with disastrous consequences, affecting 170 million people worldwide each year (Gezahegn & Suryabhagavan, 2018).

East Africa has been facing flooding problems due to heavy rainfall. Around 2.5 million people, just in Ethiopia, Sudan, and South Sudan, have been defenseless against the flood of water. At least 1.3 million people have been affected by flooding; 481,000 have been relocated; and 360 individuals have lost their lives as a result of devastating floods in the region (Kassegn & Endris, 2021). The meteorological stations in Africa indicate the highest rainfall has been gauged in the last 40 years. Over 1.3 million people have been affected by flooding in the sub-region since the beginning of the long rainy season in March 2020, including at least 481,000 displaced people. This includes people in Burundi (where over 50,000 people have been affected, the majority of whom are displaced), Djibouti (where over 110,000 people were affected in the capital in the last week of April 2020), Ethiopia (where 219,000 people have been affected, including nearly 107,000 displaced), and Kenya (where 233,000 people have been affected) (OCHA, 2020).

The major problems in Ethiopia concerning floods are inundation and bank erosion. Furthermore, a flash flood that happened in the countryside a few years ago destroyed infrastructure, washed away houses, cost many lives, and damaged agriculture. The problem is influenced by the plain's topography in the river system, flow phenomena, and land cover (Desalegn & Mulu, 2021). Ethiopia experienced 86 natural catastrophes between 1980 and 2010, costing 313,486 lives, uprooting 57 million people, and causing an economic loss of US$31.7 million (OFDA, 2012). Ethiopia generally faces two types of floods. These are floods from excessive and prolonged rainfall that contribute to the flooding of the river's main and tributaries, and floods from unexpected excess water released from reservoirs or dams (Gebre, 2015).

Floods often have a significant negative influence on society and the environment. The effects of floods include damage to property and the environment, in addition to the terrible loss of life and livelihood. In Ethiopia, rivers that overflow or burst their banks and floodplain regions downstream are attributed to flood disasters (Koriche, 2012). Urban floods can be divided into three categories: floods caused by overbank river flow, floods caused by high tides, and floods caused by storm surges. Inadequate or poor drainage contributes to urban floods brought on by heavy rainfall (Hategekimana et al., 2018). Urban areas have a large amount of impervious surface and artificial waterways. Rapid urbanization in recent decades has transformed rural areas into urban areas, and the development and expansion of impermeable areas have enabled urban runoff to increase. Significant factors that affect flood risk include changes in land use and land cover, urbanization, unregulated construction, inadequate sewerage systems, and an increased impervious surface in urban areas (Khalaj et al. 2021).

Even though a flood is a natural disaster, it can be managed by properly implementing different structural and non-structural techniques. Hence, assessing the flood vulnerability, mapping the risk zones, and inundating areas are some of the prevalent techniques used to minimize the risk of flooding these days. Thus, the GIS-based analytical hierarchy process (AHP) generated a weight of criteria through a matrix of pairwise comparison, and a flood risk map was produced using ArcGIS overlay analysis of weighted flood causative factors. Furthermore, the Super-Fast Flood Model simulated flood inundation depth. The main focus of the study was mapping the flood risk areas and computing flood inundation depth in the city using an integrated multi-parametric analytical hierarchy process (AHP-GIS) and a super-fast flood model. Therefore, this study could be helpful in flood protection, the redesigning of drainage systems by considering the highly vulnerable areas, and mitigation policies in Adama City.

1.2. Statement of the Problem

Flooding is one of the major natural disasters that has disrupted social and economic development (Guo et al., 2021). According to the WMO (2021) , floods led to the largest human losses, with about 58,700 deaths and US$521 billion in economic losses. Similarly, weather, climate, and water hazards accounted for 50% of all disasters (including technological hazards), 45% of all reported deaths, and 74% of all reported economic losses at a global level over the past 50 years.

Several flood incidences have been reported in the Afar, Oromia, SNNP, and Somali regions of Ethiopia. About 202 people were affected by the devastating floods in 2016. Recently, four people died and numerous others were injured as flash floods hit the city of Dire Dawa on April 24, 2020. More than 47 flood events have been documented in Ethiopia's historical flood records, which date back to the 1980s and affected 2.2 million people (Weldegebriel & Amphune, 2017).

In recent years, Adama City has been severely affected by flooding problems. For instance, the city has experienced significant losses as a result of the floods that occurred in 2000, 2008, 2009, and 2016. Periodic observations showed a substantial increase in the social, economic, and ecological damages caused by flooding. This is because the city does not have a comprehensive early warning system for managing flood risk. These issues call for continual improvement in analysis, mitigation, and management (Tesema, 2017).

Generally, Adama City has experienced flooding problems that have led to the displacement of communities in some areas of the sub-city, destroyed different infrastructures, washed away houses, and damaged commercial centers and buildings. Therefore, to minimize the chronic problem of flooding in the city, it needs a critical flood hazard assessment and mapping of the zones at risk to undertake the appropriate countermeasures and essential flood protection mechanisms, and it’s even essential to provide an early flood warning to vulnerable communities and elements at risk.

1.3. Objectives of the Study

1.3.1. General objectives

The general objective of this study was to assess and map flood hazard for Adama City.

1.3.2. Specific objectives

- To identify flood causing factors and generate their spatial maps.
- To analyze flood inundation depth for past flood event and future scenarios.
- To generate flood hazard map for Adama City.

1.4. Research Questions

- What are the flood generating factors in Adama City, and which criteria are highly contributing to flooding?
- How deep is the flood inundation in vulnerable areas of the city?
- Which areas of the city are at high risk of flooding?

1.5. Significance of the Study

Given the increase in flood events in recent years, accurate flood risk assessment is an important component of flood mitigation, effective flood risk management, and disaster reduction policies (Rincón et al. 2018). Ignorance of flood risk is probably responsible for almost 40% of flood damage (Marco, 1994). Flood risk maps can be used to provide baseline information for land use planning, allow proper development of new urban areas, assess flood costs and risk mitigation, appropriately assess the feasibility of non-structural flood control measures such as flood control, and provide a logical basis for investment planning and prioritization. Flood risk maps also increase public risk awareness (Marco, 1994). An urban flood vulnerability map is helpful for urban planning and expansion management (Yeganeh & Sabri, 2014).

This study generated a flood risk map, addressed the vulnerable areas, and computed flood inundation depth; furthermore, it developed an IDF curve for Adama City. The result of this study can be used in planning, designing drainage systems, and planning effective emergency responses for flood-risk areas in Adama City. Furthermore, the generated flood risk map in this study plays a vital role in the planning and construction of any projects along the city's flood risk area. The results of this study can also be an input for other studies, like those on the social and economic impacts of flood damage, that help to know how the community was affected.

1.6. Scope and Limitation of the Study

Adama City is one of the fastest-growing cities in Ethiopia and is highly affected by seasonal flooding. Even though the problems of flooding occur in different cities and towns in Ethiopia, the scope of this research is geographically and thematically delimited. Hence, Adama was selected for the case study, taking into consideration the time and resource limitations. The impact of flooding in terms of individual households and damaged infrastructure was not assessed specifically because of the requirement for intensive field data and time. This study assessed the flood vulnerability, mapped the risk areas, and computed the flood inundation depth of Adama City using an integrated multi-parametric AHP-GIS and Super-Fast Flood model. The results of flood inundation depth obtained from fast flood model were face challenges due to the lack of streamflow gauging station.

1.7.Thesis Organization

The organization of this thesis is structured five distinct chapters. In Chapter One, the groundwork for research is laid out, encompassing the introduction, background of the study, objectives, and a clear statement of the problem under investigation. Chapter Two delves into an extensive literature review, providing a comprehensive overview of the existing body of knowledge related to the subject matter. In the Chapter Three, the focus shifts towards the data sources, materials utilized, and methodology adopted to conduct the research, ensuring transparency in the research process. Chapter Four presents the culmination of the study, offering the results obtained and fostering a robust discussion around those findings. Finally, Chapter Five encapsulates the research journey, drawing conclusions from the study's outcomes and providing valuable recommendations for future endeavors in this field.

2. LITERATURE REVIEW

2.1. The Concepts of Flood

2.1.1. Flood and Flood Inundations

Flooding is a natural disaster that occurs in different countries all over the world. It is a disaster-related occurrence that happens when the water level rises higher than usual, typically during the rainy season. An area that is suddenly and temporarily submerged in water is referred to as a flood. It frequently occurs in a dry area where water does not regularly cover the ground (Sulaiman et al., 2012). A flood occurs when the capacity of the channel is insufficient to carry the flow of water and the channel overflows, thus, in turn, affecting both urban and rural areas (Desalegn & Mulu, 2021).

Flooding has a wide range of complicated impacts. These impacts include direct harm to structures and property, interruption of economic activity, and displacement of the affected people with the associated expenses of evacuating and finding temporary housing. It includes decreased agricultural output and lost opportunities, as well as significant harm to cultivation at various phases of development. It might affect populations that are not directly impacted by flood waters for long periods, not just during the period of inundation. They include direct damage to infrastructure as well as disruptions of transportation and services (Fikadu, 2012). Urban areas are more likely to be affected by inundation risk than rural areas because they are more densely populated and host critical infrastructure (Khalaj et al. 2021).

2.1.2. Causes and Types of Flood

River floods, flash floods, coastal floods, and urban floods are the most common types of floods. Floods are generally brought on by climatological factors, changes in land use, an increase in population, and land subsidence (Fikadu, 2012). Flooding can happen in a variety of ways. Among the most notable are the quick melting of ice in the highlands, intense rainfall, overflowing rivers and streams, and breaches in flood protection systems. The majority of floods build up over hours to days, except for flash floods, which only happen in the foothills. Flooding of rivers is brought on by an abundance of precipitation and/or snowmelt, which causes rivers to overrun their banks and cover land that is ordinarily dry (Hagos et al., 2022).

Fluvial (overbank) or river flooding is a normal process that is necessary for the ecosystems of rivers and floodplains to function properly. The frequency and severity of river flooding occurrences can both rise as a result of increased urbanization. Pluvial flooding occurs when the rate of rainfall in an area exceeds the infiltration rate into the ground surface. It is particularly challenging to predict pluvial flooding, which is frequently associated with localized, intense, and short rainfall events (Rubinato et al., 2019).

A flash flood is one of the most devastating natural disasters that disrupts and damages properties, social stability, and the environment. It is challenging to take action for an effective reaction to a flash flood because of its rapid onset and because it is mostly caused by heavy rain. Understanding the socioeconomic traits of societies and their susceptibility to these extreme events is necessary to build resilience to flash floods (Khajehei et al., 2020). Climate change may also worsen flood frequency and intensity (Tanoue et al., 2016). The fast response time of flash floods implies that affected populations often do not have enough time to reach out for help. In many circumstances of flash floods, individuals and subgroups protect themselves on their own without the assistance of formal risk managers (Borga et al., 2019).

2.2.Urban flooding

The problem of urban flooding has become increasingly urgent due to the effects of urbanization and climate change. The magnitude and frequency of floods are influenced by rapid urban growth, variations in rainfall intensity due to climate change, and inadequately designed drainage systems. Urban development activities that increase imperviousness reduce infiltration rates, increase surface runoff, and contribute to flooding volume (Bibi & Kara, 2023). Assessing flood risk in urban areas involves complex interactions between natural and engineered processes. The construction of impervious areas facilitates rapid surface runoff from rainfall, impacting urban flow regimes. The reduction in hydrological response time in urban areas increases fluvial flood risk, particularly in areas with high impervious surface coverage (Mehedi et al., 2022). Understanding the impacts of urban development on floods is crucial for effective flood management and reducing vulnerability. The removal of vegetation and soil, grading of land surfaces, and increasing of built-up areas alter stream channels, leading to an increased flood hazard (USGS, 2003).

2.3.Short duration rainfall synthesis for urban flood modeling

The disaggregation of rainfall data into short-duration rainfall is essential for hydrological modeling and flood risk assessment. Continuous simulation models require long-term rainfall records to generate the long-term statistical response of the hydrological system (Burian & Durrans, 2002). However, long-term rainfall records are often not available or have low temporal resolution. Therefore, disaggregation methods have been developed to distribute daily rainfall totals into individual storm events with high temporal resolution (Koutsoyiannis, 2003). Acharya et al. (2022); Basumatary and Sil (2018); Bibi (2023); Engida and Esteves (2011) study disaggregated daily rainfall data into short-duration storm rainfall. The approach utilizes a regression model to estimate the relationship between daily and hourly rainfall data and applies the model to disaggregate daily rainfall data into hourly rainfall data (Acharya et al., 2022). Overall, the disaggregation of rainfall data into short-duration rainfall is an important step in hydrological modeling and flood risk assessment, mostly in fine-resolution RF data-scarce areas.

2.4.Intensity duration frequency (IDF) curve in urban flood modeling

The intensity duration frequency (IDF) curve is a critical tool in urban flood modeling because it represents the relationship between rainfall intensity, duration, and frequency of occurrence. The curve is used to estimate the design rainfall for a given return period, which is essential for the hydraulic design of drainage system (Agonafir et al., 2023). The IDF curve is typically developed using historical rainfall data and statistical methods such as the Log-Pearson Type III, Gumbel extreme value theorem, Log-Pearson Type III distribution, and generalized extreme value distribution (Fowler et al., 2021). The IDF curve is an essential component of urban flood modeling and is used to estimate the design rainfall for various return periods, which is crucial for designing hydraulic structures and drainage systems (Fowler et al., 2021). The IDF curve is also used to assess the impacts of urbanization on flood risk by comparing the IDF curves for different land use types.

2.5.The Impact of flooding and flood controlling techniques

Flooding has been the most damaging and frequently occurring natural disaster in the world. The severity of the flood problems is further exacerbated by the lack of coordinated national and local flood disaster mitigation measures and early warning systems (Nigusse & Adhanom, 2019). The balance between the risk of the flood (hazard), the number of people or the value of assets that could be affected by flooding (exposure), and the susceptibility to harm or lack of socioeconomic capacity to deal with flood risk depending on economic, social, demographic, cultural, institutional, and governance factors can be seen in the differences in flood risk between regions. Due to historical efforts to reduce flood impacts, developed countries often experience less severe flood loss and damage than developing ones, especially in terms of the number of fatalities. Flooding has been extremely damaging to developing countries due to a lack of adequate flood protection (Tanoue et al., 2016).

Massive damages caused as a result of floods around the world have prompted action to address the flood problem as a top-priority issue. To address the issue, both structural and nonstructural measures have been implemented. Structural measures, as the name indicates, are those that include the construction of structures like dams, embankments, drainage channels, etc. However, after spending large sums on flood management work, it was realized that this technique did not work very well alone. Non-structural measures might include floodplain management, floodplain zoning, floodplain regulation, and flood forecasting, which are the most prevalent ways of flood-controlling techniques these days (Aggarwal et al., 2009).

Samuels (2006) suggested the following flood management activities for flood-prone areas:

Pre-flood activities include:

- Identify vulnerable areas.
- Planning for disasters to identify evacuation routes, public services, and infrastructural supplies for emergency activities.
- Building flood-related infrastructure (physical structure and forecasting system).
- Planning for land use and limiting inappropriate development in flood areas
- Awareness of flood exposed people

The post-flood activities:

- review of flood management strategies to advance hazard planning in the future
- Rehabilitation and reconstruction of construction of damaged places
- Economic and environmental restoration
- Relieving injuries

2.6. Flood Risk, vulnerability and Hazard

2.6.1. Flood risk

According to Lane (2017), flood risk is the likelihood of experiencing floods (the hazard) in a way that has unfavorable effects. The negative consequences may be broadly defined as the broad range of impacts on economic, social, health, welfare, etcetera., or specifically defined as economic losses that would arise from the exposure. Flood risk is the outcome of a flood hazard (Nigusse & Adhanom, 2019). Flood risk is the result of both flood vulnerabilities and hazards at a certain location. Therefore, it requires systematic variable assessment, collection, and analysis. GIS has become a crucial tool for mapping and analyzing flood hazards, as it makes it easy to generate maps of inundated areas (Nigusse & Adhanom, 2019). Flood risk is the consequence of three factors: flood hazards, exposure, and vulnerability (Lane, 2017).

Flood risk is both a result and a function of vulnerability and hazards. Flood risk can be directly related to the concept of disaster, given that it comprises all the losses and damages that might be suffered following a natural hazard: death and injury, damage to property, and suspension of activities. Risk denotes a potential future state that depends on the severity of the natural hazard and the susceptibility of all exposed elements at a given time (Ologunorisa et al., 2005).

2.6.2. Flood Vulnerability

Vulnerability refers to the potential for physical, structural, or socio-economic elements to suffer harm, destruction, or loss due to natural hazards. It's important to view vulnerability as a dynamic concept that integrates evolving changes and advancements, shaping the likelihood of damage to exposed components. This perspective is crucial since vulnerability doesn't remain static, necessitating a comprehensive understanding of the evolving risk landscape(Ologunorisa et al., 2005). Exposure, sensitivity, and reaction, or resilience, to the combined effects of both human and environmental systems make up vulnerability (Khajehei et al., 2020). One of the important factors in risk management and flood damage assessment is flood vulnerability. Vulnerability can be defined as the exposure, susceptibility, and resilience of each population in a risk situation. Since disasters are determined to be caused primarily by vulnerability, it is vital to improve how vulnerability is perceived (Nasiri et al. 2016).

2.6.3. Flood hazard

Hazard is the likelihood that during a specific time period in a specific location, a very intense and potentially harmful natural phenomenon will occur that induces air and earth movements that will have an impact on that place. The extent of the phenomenon's impact, its probability of occurring, and its scale can all be determined in particular circumstances (Ologunorisa et al., 2005). The characteristics of the flood occurrence in terms of magnitude and frequency are considered in the hazard assessment (Nigusse & Adhanom, 2019).

2.7. Flood Disaster in Ethiopia

80% of the rainfall in Ethiopia is received in June, July, August, and September. Large-scale flooding in Ethiopia mostly occurs in the lowland areas where major rivers flow into neighboring countries because of the country's fairly rugged topography and clearly delineated watercourses. However, heavy rains in the highlands could result in the flooding of towns near any river course (Wondim, 2016). The Awash river basin is one of the twelve main river basins of Ethiopia and has been experiencing severe annual flooding. The Wabi Shebelle River in southeast Ethiopia, close to the Somali border, and the Baro Akobo/Sobat River in western Ethiopia, close to the Sudanese border, are the other rivers that experience considerable flooding. About 300,000–350,000 ha of the Baro Akobo flood plain and 100,000 ha of the Wabi Shebelle basin are subject to annual flooding. Integrated water resources management in Ethiopia is still in its early stages (Achamyeleh, 2003). Several urban areas in Ethiopia have experienced severe flood disasters in recent years due to urban growth and climate change. The impact and severity of floods will be exacerbated due to insufficient urban drainage systems and poor urban storm water management (Jemberie & Melesse, 2021).

2.8.Flood Hazard factors

Surface runoff manifests as a flash flood if the intensity of the rainfall is greater than the soil's capacity for infiltration and evaporation. Rainfall on impermeable surfaces, such as roads and other paved places, also causes it to happen. There are several factors that affect the identification and modeling of flood hazards. Runoff, surface slope, elevation, land use land cover (LULC), soil influences, surface roughness, drainage density, and distance from the river are some of the flood causative factors mostly used in flood hazard mapping (Elkhrachy, 2015).

A weighted sum overlay of slope, elevation, drainage density, land use and cover, and developed factors was used to generate a flood risk map (Wondim, 2016).

2.9.Flood Risk Assessment and Mapping the Hazard Zones

Risk assessment is a crucial step in risk management and reduction in the broadest sense (Phongsapan et al., 2019). For the projection of future flood risks and the development of efficient flood mitigation strategies, an understanding of the physical and spatiotemporal properties of flood causative factors is crucial (Tanoue et al., 2016). It is necessary to properly locate areas that are prone to flooding and waterlogging to predict and assess the spatial distribution of floods in the future (Wang et al., 2015). An inundation hazard map shows the area at risk for inundation and delineates the hazardous locations where inundation events are likely to occur (Khalaj et al., 2021). Various types of information, such as satellite-derived data products and statistical data compiled by region, are used to calculate flood risk. The majority of data layers have been standardized to enable qualitative comparisons between data from various sources. The final flood risk index is created by combining the various data layers necessary to compute the hazards, exposures, and vulnerabilities. The risk map, which aggregates risk values for a region, is used to construct the flood risk index (FRI). The final risk map is obtained by multiplying the flood hazard, flood exposure, and flood vulnerability indices (Phongsapan et al., 2019).

Flood hazard zone map is used as non-structural flood control mechanism, planning of the flood plain and for policy makers in the regulation of developmental activities along the flood plain and the zones at risk of flooding. For basins that experience frequent flooding, a flood hazard zone map can be created using historical satellite data in conjunction with hydrological and close contour data (Aggarwal et al., 2009).

2.10. Application of GIS and RS in Flood Hazard mapping

Remote sensing technology advancements and geographic information systems (GIS) for real-time monitoring, early warning, and rapid assessment of flood disaster damage. The Geographic Information System is a tool that can help floodplain managers locate places in their area that are vulnerable to flooding. Geographical information is stored in a database with a GIS, where it can be queried for and graphically displayed for study. Different geographical layers can be overlaid or intersected to identify flood-prone areas and prioritize them for mitigation or more rigorous floodplain management activities (Aggarwal et al., 2009). Remote sensing can be effectively utilized for mapping flood damaged areas (Phongsapan et al., 2019). Remote sensing can be effectively utilized for mapping flood-damaged areas (Morea & Samanta, 2020). GIS and remote sensing techniques have emerged as powerful tools for dealing with different aspects of flood management, including prevention, preparedness, and relief management of flood disasters. For various floodplain management tasks like base mapping, topographic mapping, and post-disaster validation of mapped floodplain extents and depths, GIS is best suited. The current flood control system can be replaced, enhanced, or improved with the help of remote sensing and GIS tools. The creation of long-term databases on flood proneness, risk assessment, and relief management has significant potential if these technologies are used extensively (Aggarwal et al., 2009).

2.11. Analytical Hierarchy Process (AHP)

AHP is an MCDA tool that assists decision-makers in setting priorities and drawing better conclusions when dealing with complex decision-making. Overall, the GIS-based MCDA-AHP technique for assessing flood risk has proven to be effective. It incorporates many flood-causative elements and criteria into the GIS analysis tool to produce superior flood risk maps (Morea & Samanta, 2020). The analytical hierarchy process is a helpful tool that may be used in order to select the best conceptual design. AHP has been used in virtually all applications involving decision-making issues (Ariff et al., 2008). The analytical hierarchy process is a tool for making decisions based on several factors. This pair-wise comparison method uses Eigen values. Additionally, it offers a way for calibrating the numerical scale used to quantify both qualitative and quantitative performance. The comparison's complete range is covered by the scale, which goes from 1/9 for "least valued than" to 1 for "equal" and 9 for "absolutely more important than" (Saaty, 1980).

In the past, hydrologic and hydraulic models were widely employed to predict possible flood damage and inundation zones for specific recurrence intervals. These models essentially only take into account how waterways' flow and transportation are balanced. The AHP-based method of assessing flood risk is cost-effective, simple to apply, and, most importantly, allows interactive usage by flood planners for ongoing development. Understanding the factors generating floods on the flood plains would be made easier for flood managers and local community leaders with the aid of an AHP-based flood risk assessment (Chen et al., 2011). AHP offers a powerful quantitative decision-making tool to handle complicated and unstructured problems by organizing and evaluating alternatives in relation to a hierarchy of multifaceted attributes. AHP provides a better, simpler, and more effective framework for selecting criteria, determining their weights, and analyzing the results (Bojovic & Milenkovic, 2008).

The nine-level standardized comparison scale serves as the foundation for multiple pairwise comparisons in AHP, as shown in Table 2.1. Psychologists have shown that nine objects are the maximum number that a person can consistently compare and rank at the same time. The best information that is available, along with the decision-maker's knowledge and experience, are used to make pairwise decisions (Schoenherr et al., 2008).

Table 2.1. Nine-point intensity of importance scale

Intensity of importance	Definition	Description
1	Equally important	Equal contribution
3	Moderately more important	slightly favor one over the other
5	Strongly more important	strongly favor one over the other
7	Very strong more important	very strongly favor one over the other, demonstrated in practice
9	Extremely more important	The evidence favoring one over the other is of the highest possible validity
2,4,6,8	Intermediate values	When compromise is needed
Reciprocal of above	The element compared with the assigned one	
Ratios(1.1-1.9)	If the activities (elements) are very close	May be difficult to assign the best value

The following scale of absolute values (not ordinals) must be used in the judgment phase of the analytic hierarchy process (AHP) to communicate judgments while doing paired comparisons: 1, equal; 3, moderate; 5, strong; 7, very strong; 9, extreme; 2, 4, 6, and 8 are compromise values, reciprocals for the inverse comparison, and decimal modifications between if a preset set of final priorities is needed (Saaty, 1987).

2.12. Integration of AHP and GIS for flood Hazard mapping

Remote sensing technologies and GIS-based spatial analysis approaches are helpful for mapping flood risk and other hazards, providing an alternative to conventional survey methods. A fundamental framework or platform that supports hazard assessment and management at all stages, from preparation to response and recovery, can be easily obtained using GIS and remote sensing techniques. Multi-criteria decision analysis (MCDA) helps decision-makers organize complex alternatives effectively and evaluate their many alternatives. AHP is an MCDA tool that assists decision-makers in setting priorities and drawing better conclusions when dealing with complex decision-making. Overall, the GIS-based MCDA-AHP technique for assessing flood risk has proven to be effective. It incorporates many flood-generating elements and criteria into the GIS analysis method to generate favorable flood Hazard maps (Morea & Samanta, 2020).

Through using longer rainfall and flood data, adding more components and categorizing those elements into more risk categories, and improving the AHP methodology through iterative collaboration with experts, further advancements in the flood risk assessment using the AHP/GIS method can be made. AHP and GIS integration could offer a more thorough and insightful assessment of flood hazard, as well as an interactive assessment with the decision makers (Chen et al., 2011).

2.13. RFI and IDF Curve

The intensity duration frequency (IDF) curve is a critical tool in urban flood modeling. The IDF curve represents the relationship between rainfall intensity, duration, and frequency of occurrence (Agonafir et al., 2023). The curve is used to estimate the design rainfall for a given return period, which is essential for designing hydraulic structures and drainage systems (O’Donnell & Thorne, 2020). The IDF curve is typically developed using historical rainfall data and statistical methods such as the Log-Pearson Type III distribution, Gumbel extreme value theorems, generalized extreme value (GEV) theorems, and so on (Fowler et al., 2021).

Rainfall intensity is a crucial factor in urban flood management. Studies have shown that global climate change and rapid urbanization will further increase the frequency and intensity of urban flood disasters (Zhao et al., 2023). The results of recent research indicate that urban flood volume increases non-linearly with increasing rainfall intensity under climate change (Sun et al., 2021). To effectively mitigate future flood risks, it is crucial to combine a comprehensive examination of intense rainfall events in urban areas with the utilization of urban flood modeling (Iliadis et al., 2023). Urban growth also plays a role in the resilience of communities at flood risk, as it can impact the urban drainage system and increase the vulnerability of urban areas to flooding (Hemmati et al., 2020). Overall, understanding the relationship between rainfall intensity and urban flooding is essential for designing effective flood management strategies and mitigating the impacts of flooding in urban areas (Agonafir et al., 2023b).

2.14. Superfast Flood Model

The present level of technology for real-time, complete flood simulations across vast geographical regions is poor. This limitation affects warning systems, interactive planning, and detailed predictions. Consequently, the general public cannot receive information about the paths of significant water masses quickly and reliably. The Super-Fast Flood (SFF) web based model calculates flood risk maps significantly faster than existing cutting-edge techniques by utilizing steady-state flow principles (van den Bout et al., 2023).

Van den Bout et al. (2023) tested the SFF model across five different study areas and observed a substantial average reduction in computational costs by a factor of 1500. This achievement introduces a new outlook to the realm of flood hazards, enabling novel approaches to flood risk mitigation through innovative early-warning systems and interactive hazard assessment tools. As climate change is certainly anticipated to aggravate flood hazards, the SFF method provides the potential to significantly enhance the efficiency of flood simulations, thereby contributing to the preservation of lives and livelihoods.

The SFF model has demonstrated similarity to fully dynamic water flow simulation across various events, including the extreme 2003 floods in the Fella Basin (Italy), Hurricane-induced flooding on Dominica, and the flood impact in Limburg in 2021 (The Netherlands). On average, the calculation time decreased from approximately 6 hours to 2.5 minutes while maintaining a high degree of accuracy. The model's sensitivity to initial conditions was similar to that of conventional flood models, but its sensitivity to hydraulic aspects is comparatively lower (Bout, 2022).

2.15. Previous Studies on Flood Vulnerability, Hazard Mapping and flood inundation

There are various studies regarding flood inundation, hazard exposure, assessment, and risk mapping with different methodologies and data types and different aims around the world and specifically in Ethiopia.

Chen et al. (2011) integrated AHP and GIS to map the relative flood risk of the Fazih River floodplain, developed the AHP hierarchical structure using seven flood causative factors, and finally concluded that the integration of the analytical hierarchy process and GIS in flood risk assessment can provide detailed information regarding flood risk management. Tesema (2017) employed a multi-criteria approach to evaluate the flood risk map of Adama City. The findings show that 10.4% of the city's total area is in a high-risk zone and that the ecological flood risk in the city is most evident in the southern section of the city. Low drainage density, low elevation, and the imperviousness of the land area are the main causes of this, but the author did not use sufficient data, which helps to conclude the study's result. Flow accumulation, annual rainfall, slope, runoff, LULC, elevation, geology, soil type, distance from the drainage network, and drainage density were the 10 flood hazard factors that were used by Mahmoud and Gan (2018) to create flood susceptibility maps for the Riyadh province in the center of Saudi Arabia. The province's northern, northeastern, and northwest regions have the highest flood vulnerability zones, and the author recommended employing at least six flood causative factors to map the flood risk zones.

Desalegn & Mulu (2021) assessed flood vulnerability in the Fetam watershed of the upper Abay basin using multi-criteria evaluation and GIS, considering flood causative factors such as land use and land cover, slope, rainfall, soil type, drainage density, and elevation to mark out flood-prone areas of the watershed. The author presented a flood vulnerability assessment map of the areas with very high, high, moderate, low, and very low flood risks, which correspond to 67.54, 634.11, 280.89, 121.28, and 2.81 km^2, respectively. Along with the flood danger zones, which are prone to flooding, are residential areas and agricultural fields. Because of the fatalities and damage to residents' properties, the localities are vulnerable to social and economic development. Gebre (2015) utilized MCDM techniques with GIS and HEC-RAS and marked out the flood inundation areas and flood risk map. In comparison to the downstream part, the upper and middle Awash Basins have less inundated regions. Additionally, the author suggested that afforestation and proper land use management are important to lessen the negative effects of floods, especially in low-lying flood-prone areas.

Hagos et al. (2022) employed the integration of AHP and GIS to assess the flood hazard zone of the Teji watershed in the upper Awash basin by analyzing different flood-generating parameters such as soil type, drainage density, slope, proximity to the river, RF, LULC, and elevation. The result inferred that 43% of the Taji watershed is highly affected, while 13.09% is subjected to extremely high flooding. Finally, the authors suggested that a periodic and sustainable implementation of food prediction, early warning, and management strategies could be achieved. Wondim (2016) analyzed flood causative factors, namely slope, drainage density, elevation, LULC, and soil type, in a GIS environment and produced the weighted relative flood risk map of the lower Awash sub-basins. The result showed that 39% and 33% of the area are subjected to high and very high flood hazards, respectively. Furthermore, the author stated that in the Lower Awash Sub-basin, there are towns, kebele centers, and settlements that are at high risk of flooding. To reduce the risk of future flooding, immediate attention must be given to such settlement areas.

Generally, flooding is one of the most serious natural disasters in the world, specifically in Ethiopia. Furthermore, Adama City has been encountering flooding problems almost every year, with varying scales. Thus, the assessed flood vulnerability, the mapped risk zone, and the computed flood inundation depth are essential to minimize the risk of flooding and give an effective post-flood response. The measurement of flood depth and inundation at every point and throughout the entire city is too long and costly. Hence, it’s better to go through other options to minimize the risk that arises due to flooding. Various studies have shown that it is very good to use AHP-GIS for an in-depth understanding of urban flooding because AHP allows for a detailed knowledge of flood causative factors in specific areas through assigning weights to each criteria. In this study, the implementation of the AHP-GIS with a super-fast flood (SFF) model showed very good results towards understanding the flooding problem in Adama city. The results obtained from this study correctly identified the flood risk index (FRI), marked out flood risk zones, and computed flood inundation depth in vulnerable areas of the city.

3. MATERIALS AND METHODS

3.1. Study Area

Adama City is one of the fastest-growing cities in Ethiopia and is located in the Awash Basin Rift Valley. The city was founded in 1916 along the Addis Ababa to Harar road, at a distance of approximately 96 kilometers, on features of flat terrain and surrounded by plateaus, mountainous terrain, and ridged topography. It is located between $8^0$26’15" and $8^0$37’00" N and $39^0$12’15" and $39^0$19’45" E. The area's altitudes range from 1475 m to 1970 m above mean sea level. The average annual RF of Adama City is 866.25mm. In the rainy season (June to September), most of the rainfall occurs. September has the lowest wind speed (1.65 m/s), while December, January, and February have the highest wind speeds (3.05–3.2 m/s). The city's average temperature ranges from 11.5^0C to 3^0C. The flat-lying rift in which Adama City is located and the city's impervious surface make flooding a severe natural hazard there (Bulti & Abebe, 2020).

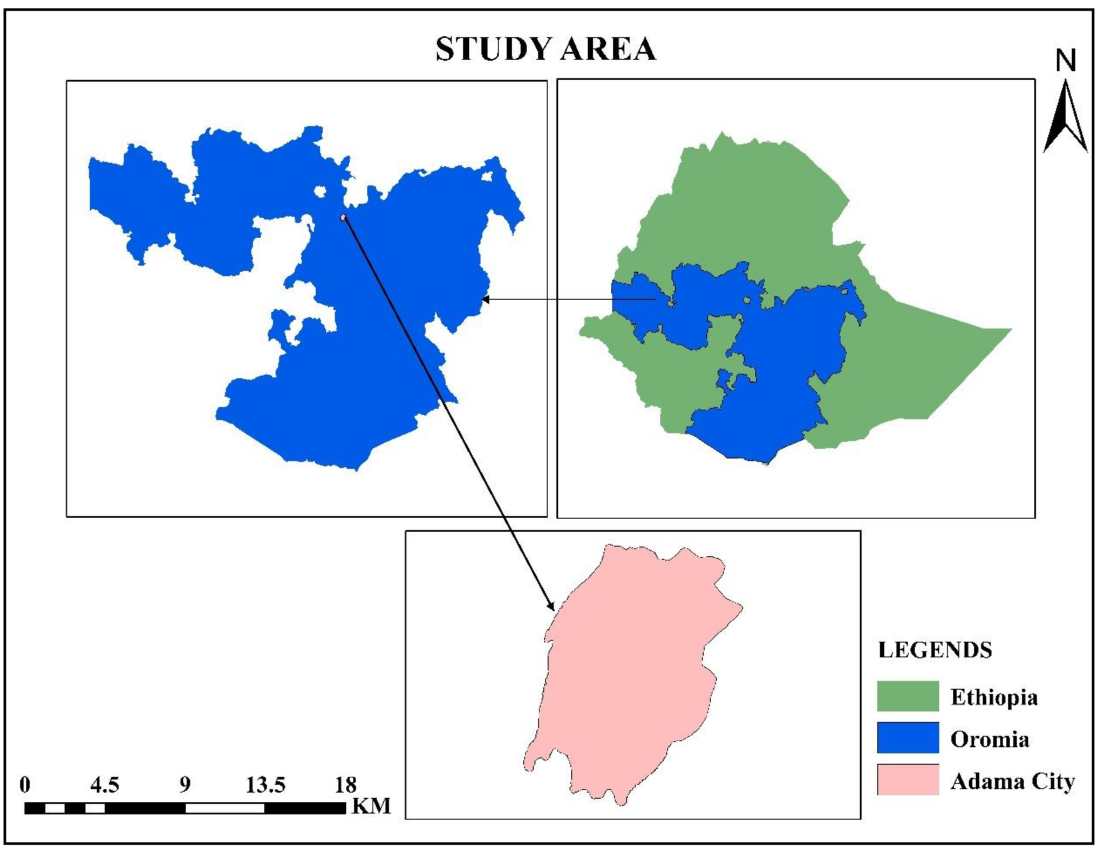

Figure 3.1 Location map of study area

3.2. Data Collection

The data used for this study includes spatial (digital elevation model, land use and land cover, drainage network, road network, storm drains, and soil type) data used to create raster layers, daily data of climatic variables (precipitation) and CHIRPS spatial rainfall, experts and local resident's questionnaires, and interview data, respectively. All data were gathered from secondary sources except for an interview with experts and local residents in the city. PCP, DEM, road network, LULC, drainage network, storm drains, and soil map data were used to obtain a weighted flood risk map and for simulation of the Super-Fast flood model, whereas experts and local residents interview responses were used in the pair-wise comparison judgmental process and validation of results.

3.3. Data Type

The types of data used in this study and their respective sources are depicted in Table 3.1.

Table 3.1. data types and their sources

Data type	Data's	Sources
Meteorological data	PCP	Adama meteorological station
	Monthly CHIRPS PCP(1990-2022)	https://data.chc.ucsb.edu/products/CHIRPS-2.0/africa_monthly/tifs/
Geo-physical data	DEM	https://search.asf.alaska.edu/
	LULC	Sentinel-2, (https://eos.com/landviewer)
	Soil data	FAO (Food and Agriculture Organization)
Road and drainage related data	Road networks	Adama City Municipality
	Drainage network	
	Storm drains	
Qualitative data	Information from local residents	Interview
	Information from experts	Questionnaire

3.4. Materials Used

Table 3.2. Materials and software used in this study

Types of Software/Tools	Purposes
GIS	Preparing the study area, creating raster layers, performing overlay analysis, and obtaining a weighted flood risk map
AHP	For pair-wise comparison of flood causative factors and to identify the relative importance of employed parameters and the city's flood risk index
SFF model	To determine flood inundation depth and its extent
MS-Excel	Used for categorizing and handling data
HEC-SSP	For frequency analysis of rainfall events

3.5. Data Analysis

The analysis of the data used in this study is discussed as follows:

3.5.1. Fundamental approach of AHP and pairwise comparison

A pairwise comparison technique is employed in the AHP implementation to determine the criteria's relative importance to accomplishing the aim. The priorities for the alternatives (i.e., the competing alternatives within consideration) are also determined through pairwise comparisons based on how well they performed against each criterion. Thus, the three guiding concepts of AHP are decomposition, comparative judgment, and priority synthesis (Saaty, 2008). Schoenherr et al. (2008) summarized AHP in four basic steps, such as developing the decision hierarchy, calculating the relative importance of attributes and sub-attributes, assessing each alternative and estimating its overall weight in relation to each attribute, and finally examining the consistency of the subjective judgment. AHP is an ideal methodology for specific prioritization problems by taking different criteria into account because it can handle both qualitative and quantitative data. The bellows are a mathematical illustration of the ideal methodology of AHP that was utilized in this study.

Let $c = \{C_j \mid j = 1,2,3, \dots, n\}$ be the set of criteria. The result of pairwise comparison on n criteria can be summarized in an $(n \_ n)$ evaluation matrix A in which every element

$a_{ij}(i, j = 1,2,3, \dots, n)$ is the quotient of weights of the criteria, as given in Equation 1 (J.-J. Wang & Yang, 2007).

$$A = \begin{bmatrix} a_{11}a_{12} & . & a_{1n} \\ a_{21}a_{22} & . & a_{2n} \\ . \quad . & . & . \\ a_{n1}a_{n2} & . & a_{nn} \end{bmatrix}, a_{ii} = 1, a_{ji} = {}^{1}/_{a_{ij}}, a_{ij} \neq 0 \qquad \text{Equation 1.}$$

The mathematical procedure to normalize and determine the relative weights for each matrix starts at the last stage of AHP. The right eigenvector *(w)*, which corresponds to the highest eigenvalue (λmax) as in Equation 2 (J.-J. Wang & Yang, 2007).

$$\boldsymbol{A_w = \lambda_{max}} \qquad \text{Equation 2.}$$

The matrix A has rank 1 and $\lambda_{\text{max}} = n$ if the pairwise comparisons are fully consistent. In this situation, normalizing any of the rows or columns of A will give weights. It should be noted that the consistency of the pairwise comparison assessments has a direct correlation with the output quality of the AHP. The relationship between the entries of A: $a_{ij} \times a_{jk} = a_{ik}$ defines the consistency. Consistence index (CI) is obtained by Equation 3 (J.-J. Wang & Yang, 2007).

$$\boldsymbol{CI = (\lambda_{max} - n)/(n - 1)} \qquad \text{Equation 3.}$$

The ultimate consistency ratio (CR), determines the consistence of evaluation and its value is obtained by ratio of consistence index (CI) and the random index(RI) as in Equation 4.

$$\boldsymbol{CR = CI/RI} \qquad \text{Equation 4.}$$

The maximum threshold value of consistence ratio (CR) is 10%, and if it is exceeded, a three-step process is followed (Saaty, 2008): The most contradictory judgment in the decision matrix should be identified, changing the range of values to lessen the associated inconsistency, and then the decision maker should be requested to review the judgment at a "reasonable value". The CI of a reciprocal matrix produced at random are averaged to get the random index in Table 4 (Saaty, 2008).

Table 3.3. random index (RI) used to compute consistency ratio (CR)

N	1	2	3	4	5	6	7	8	9	10
Random Index (RI)	0	0	0.58	0.90	1.12	1.24	1.32	1.41	1.45	1.49

The consistency indicator can be used to assess both the overall hierarchy's consistency and the consistency of decision-makers. The analysis of flood causative factors was undertaken using

AHP to determine the relative importance of each parameter and to make an input for GIS overlay analysis and flood risk mapping of Adama city in general.

3.5.2. AHP-GIS approach in flood Hazard mapping

Flood vulnerability mapping is a technique for calculating the degree of flood susceptibility. The process involves the selection of different flood-causative factors for an area. This process results in a multi-criteria and multi-parametric decision-making problem (Ouma & Tateishi, 2014). The benefit of MCE is the integration of a variety of decision-making alternatives in the context of multiple criteria and multiple objectives. The planners and managers of the city can make better decisions when it comes to flood vulnerability analyses by integrating GIS and MCDA. This is because MCE aggregates the assessment variables into a flood vulnerability index, and GIS makes it possible to compute the assessment factors. GIS was employed in this study to weight the AHP-evaluated data and generate the criteria maps and data layers, as well as perform spatial analysis based on the linear combination method as in Equation 5.

$$\boldsymbol{LC = \frac{1}{n}\sum_{i=1}^{n} D_i W_i} \qquad \text{Equation 5.}$$

whereas *LC* = linear combination; *Di* = decision parameter; *Wi* = *AHP* weight; *n* = numbers of parameters.

After linear combination of the elements using Equation (5) relative weight for each parameter are computed through normalizing eigenvector of the decision matrix. Afterward, GIS overlay analysis was utilized to generate the Adama city flood risk index (ACFRI) using Equation 6.

$$\boldsymbol{FRI = \sum_{i=1}^{N_2}\left[\left(RIW_i{}^2\right) + \left(RIW_{ij}{}^3\right)\right]} \qquad \text{Equation 6.}$$

whereas N_2 = the number of level 2 decision factors, $RIW^2{}_i =$ relative importance weight of level 2 decision factor *i*, and $RIW^3{}_{ij} =$ relative importance weight of level 3 sub-factor *j* of level 2 decision factor *i*.

The computed FRI was used to show critical flood-prone zones, and the flood risk map of the city was classified into five risk classes such as "insignificant," "very low", low, medium, and "very high", depending on the FRI indicators derived for the different zones of the city and shown as comparative measurements. In this study, five risk classes and eight flood-causing elements were used to rank each criterion, and each criterion under evaluation was ranked in the preferred order of the decision makers. Every element was weighted according to the projected significance of flooding and expert's views in order to obtain criterion values for each evaluation unit. Some of these factors were ranked in reverse, with weights of 1 indicating the least important and 5 indicating the most significant factor. A normalization of the raw data is typically needed to make the different criterion maps comparable. Linear scale transformation (LTS) was used for standardization. After standardization, scales 0 and 1 will be assigned to the lowest and highest standardized scales, respectively. Finally, a flood hazard map was obtained using GIS overlay analysis.

3.5.2. Analysis of Flood Causing Parameters

Flood hazard mapping using AHP-GIS requires various important flood causing factors in order to obtain an accurate map from weighted overlay analysis. Hence, eight flood causative parameters, namely rainfall, slope, elevation, LULC, road network, drainage density, storm drains, and soil map, were used in this study.

Rainfall raster

The spatial variability of rainfall has a significant impact on the generation of flood hazard map. Rainfall cannot abruptly infiltrate as groundwater, i.e., runoff. Rivers overflow as a result of the increased river discharge caused by the heavy rain (Rimba et al., 2017). Heavy rainfall is one of the main causes of floods. Flooding typically happens after heavy rain when natural watercourses or drainage channels cannot convey the extra water. Extreme rainfall is linked to floods; any water that cannot instantly soak into the ground flows down the slope (Ouma & Tateishi, 2014). The CHIRPS monthly rainfall data for 1990-2022 years were used in this study, the CHIRPS monthly rainfall data for 1990–2022 years were imported into ArcGIS. The 33 separate raster layers were created, one for each year, and the sum of the monthly rainfall for each pixel in each layer was calculated. Then, each pixel's accumulated rainfall was divided by 12 to obtain the average monthly rainfall for each year. After that, the 33 yearly layers were merged into a single raster layer using the "Mosaic to New Raster" tool. Lastly, the "Cell Statistics" tool with the "Mean" function was applied to calculate the average annual rainfall for the entire period. Then, it was classified into equal raster cells, standardized into five scales according to the spatial rainfall distribution, and finally ranked according to its importance in generating floods in the city.

Slope

Slope is a crucial sign of surface zones, which are very vulnerable to flooding. The slope plays a significant role in controlling the length and velocity of water flow. Compared to areas with steeper surfaces, areas with flatter surfaces have a higher flood risk because water moves more slowly, collects longer, and accumulates around (Ogato et al., 2020). The slope raster map was generated from a digital elevation model (DEM) in an ArcGIS environment using percent measurement. The generated raster slope map was further reclassified into 1 to 5 scales according to its significance in causing the flood.

Elevation

Elevation has a critical function in regulating the direction of the overflow and the depth of the water level (Gigović et al., 2017). The 12.5m × 12.5m resolution DEM of the city was resampled to 10m × 10m cell resolution and further reclassified into five equal raster cells using linear scale transformation (LTS) to produce an elevation raster map of the city. Finally, the raster map was ranked on a 1 to 5 scale according to its significance in causing the flood.

Land-use land-cover

LULC refers to a region's farmland, grassland, shrub land, built-up, and forestland distribution as well as the type of soil deposits. A watershed's LULC contributes significantly to the flow of floodwaters by obstructing, slowing down, or accelerating surface flow. The watershed's LULC affects infiltration rates, how surface and groundwater interact, and debris movement. Based on its capacity to either speed up or slow down the frequency of floods (Arya & Singh, 2021). Changes in LULC frequently alter the hydrological balance in urban areas, causing water to flow faster and more unpredictable, overwhelming drainage systems, and increasing the frequency and severity of flash flood disasters (Chow et al., 2016). LULC for this study was obtained from Sentinel-2 (https://eos.com/landviewer) with 10m × 10m spatial resolution and converted to a raster layer according to the land use and land cover type. Finally, a weighted LULC map was obtained using the ArcGIS environment, which was used in GIS overlay analysis to generate a weighted flood hazard map.

Drainage Density

Drainage density is a main point in hydrologic analysis and is the ratio of drainage length to the city's area. Drainage density (DD) is affected by the ability of surface materials to erode, permeability, vegetation, and slope. Inadequate drainage in the city area causes overland flow (Rimba et al., 2017). Urban areas can experience flooding due to ineffective storm drainage systems that fail to adequately channel and manage excess rainfall, causing water to accumulate on streets and other properties (Yazdi et al., 2017). In this study, DD was taken into consideration since it is one of the factors that affects the generation of floods in the city. The drainage network was obtained from Adama City Municipality, and the drainage density of the entire city was calculated in ArcGIS using Equation 7. The calculated drainage density was converted to a raster map of 10m × 10m raster cell size and further reclassified into five scales according to their density over an area of the city.

$$\boldsymbol{DD = {}^{L}/_{A}} \qquad \text{Equation 7.}$$

Whereas, DD = drainage density; L = length of drainage channel (km); A = total area of the city (km^2).

Road network

Urban road networks have an impact on the natural hydrological cycle, which can cause flooding in urban areas. As cities grow and develop, there are more impermeable surfaces like roads, pavements, and buildings, which reduce the amount of precipitation that seeps into the ground. Instead, precipitation quickly accumulates and flows over impervious surfaces, overwhelming storm-water drainage systems. The drainage infrastructure may not be able to handle the additional runoff from urban roads during periods of severe rainfall, leading to flash floods and waterlogging in low-lying areas (Singh et al., 2018). The road network of Adama City was taken from the city’s municipality, and road density was calculated using Equation 8. The raster map of road density was then prepared in an ArcGIS environment with a 10m × 10m raster cell, and the generated map was standardized and reclassified into five scales according to their density over an area of the city.

$$RD = {}^{L}/_{A} \qquad \text{Equation 8}$$

Whereas, RD = Road density; L = length of Road (km); A = total area of the city (km^2).

Storm drains

Urban storm drains are crucial for mitigating flash flooding in cities. The potential severity of flash flooding is greatly influenced by the density of storm drains in urban areas. The ability of the system to quickly collect and carry rainwater away from streets and impervious surfaces during rainfall events can be improved by increasing the density of storm drains. This reduces the risk of water accumulating in low-lying areas, minimizing the chances of flash floods. Conversely, areas with inadequate or low-density storm drains are more susceptible to urban flash flooding as they lack the necessary infrastructure to efficiently handle the increased runoff (Singh et al., 2018).

The storm drain shape file point data was taken from the city's municipality, and then a storm drain density map was generated in an ArcGIS environment using the kernel density tool. The generated storm drain density map was then converted into a 10m × 10m raster map and further reclassified into five standard scales according to their density over an area of the city.

Soil type

The area's capacity to retain water and the rate at which precipitation infiltrates are both greatly influenced by the type of soil present. Therefore, it may be regarded as one of the crucial elements in determining flood-prone areas. Sandy soils have higher saturated hydraulic conductivities than soils with finer-grained textures due to the larger pore space (Hagos et al., 2022). In this study, soil type data was analyzed on the basis of infiltration capacity. Thus, the soil data was classified into five classes based on their infiltration rates or soil texture. Afterward, the weighted soil map for Adama City was generated using the ArcGIS environment.

3.5.3. Short duration rainfall and IDF curve

Disaggregation of daily rainfall data into short-duration rainfall is important for various applications such as hydrological modeling, water management, and weather forecasting. Fine-temporal resolution data allows for a more detailed analysis of rainfall patterns and can provide valuable information for these applications (Maidment et al., 2017). However, access to reliable and continuously updated rainfall data at fine temporal scales is often lacking, especially in data-scarce regions (Massari et al., 2020).

T. Bibi (2023) used IMD methods to drive short-duration RF from daily RF data for the urban drainage design of Robe Town, Ethiopia. Engida and Esteves (2011) disaggregated daily RF into short-duration rainfall in the Blue Nile River basin, Ethiopia. Beyene et al. (2019) disaggregated daily RF data into short-duration rainfall using the Hyetos rainfall disaggregation model. Atanaw and Beyene, (2016) used the ERA method to generate short-duration RF and developed an IDF curve. In this study, the IMD technique was directly used for driving short-duration rainfall from daily rainfall data to prepare an input for the simulation of a super-fast flood model and develop an IDF curve for the Adama city.

The HEC-SSP model was used to check the fitness of an analytical distribution to a precipitation time series, which can be used to estimate the frequency of rainfall events of different magnitudes. The best probability distribution method for Adama RF event frequency analysis was selected using standard product moments by considering the test statistics values of both Kolmogorov-Smirnov and Chi-Square test statistics techniques. Hence, the results of test statistics showed that the generalized extreme value (GEV) distribution was the best fit for Adama RF event frequency analysis, as shown in Appendix Figure1, 2, and 3. The event rainfall frequency analysis was therefore conducted by the GEV distribution method using Equation 8.

$$R_{RT} = \mu - \left({}^{\delta}/_{\varepsilon}\right) * \left(1 - (-\varepsilon * R_t)\right)^{(-\varepsilon)} \qquad \text{Equation 8}$$

Whereas;

- R_{RT} is Rainfall depth at R_t

- R_t is Return period

- $Location\ (\mu)$ = 52.89, $Scale\ (\delta)$ = 10.92, $Shape(\varepsilon)$ = 0.01: these values were obtained using HEC-SSP statistical analysis.

The RF depth was forecasted for 2, 10, 25, 50, and 100-year return periods using Equation 8 for the IMD short-duration RF of Adama station.

3.6.Input preparation for super-fast flood model

The super-fast flood web-based model was simulated to determine the flood inundation depth and extent using rainfall events in Adama City. Rainfall intensity, elevation data of 10m × 10m resolution, land use land cover raster maps, and soil raster maps were used to run urban flooding using a super-fast flood model.

3.6.1. Rainfall Intensity

The highest daily peaks of the 1993–2022 years were analyzed to select the highest RF event, as shown in Figure 3.2, and the highest RF event from 1993–2022 was 99.8 mm, which rained on July 18, 2000. The Indian Meteorological Department (IMD) was used to drive short-duration rainfall for 5, 10, 15, 15, 30, 60, 120, 170, and 1440 minutes. Using Equation 9, Finally, the short-duration RF obtained from this method, corresponding to July 18, 2000, daily peak RF, was used to run the urban flood module of the super-fast flood model.

$$P_t = P_{24}({}^{t}/_{24})^{1/3} \qquad \text{Equation 9}$$

Whereas;

- P_t is the required rainfall depth in mm at t-hr duration

-P_{24} is the daily rainfall in mm

- t is the duration for depth of rain required in hr

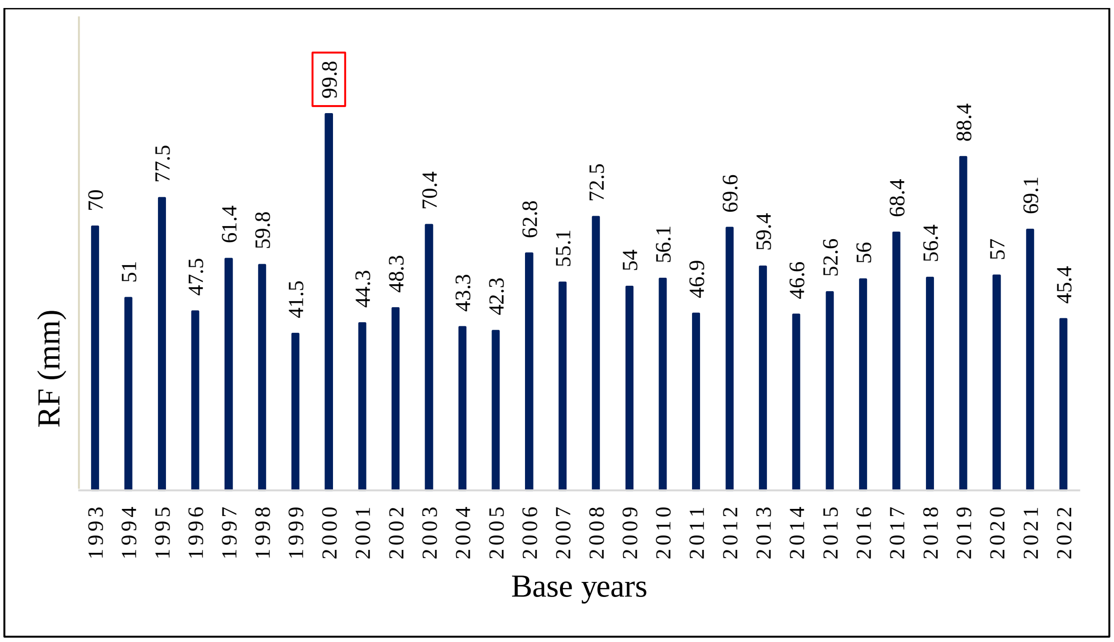

Figure 3.2. Highest daily peaks from (1993-2022) in mm

3.6.2. Manning roughness

The Manning roughness coefficients play a crucial role in hydrodynamic modeling. In this study, these coefficients were used based on Arcement et al. (1984) and Papaioannou et al. (2018) studies, taking into account the specific land use and land cover characteristics of Adama City. The approach involved referencing Table 3.4, which provided Manning coefficient data for different land use and land cover types. The practical implementation of these coefficients can greatly enhance the accuracy of hydraulic simulations and flood predictions. The relationship between the coefficients and the urban landscape is shown in Figure 3.3.

Table 3.4. manning roughness constant

Land use type	Manning roughness coefficient
Bare ground	0.025 – 0.050
Built area	0.010 – 0.050
Crops	0.020 – 0.050
Dense vegetation	0.045 – 0.080
Range land	0.025 – 0.035

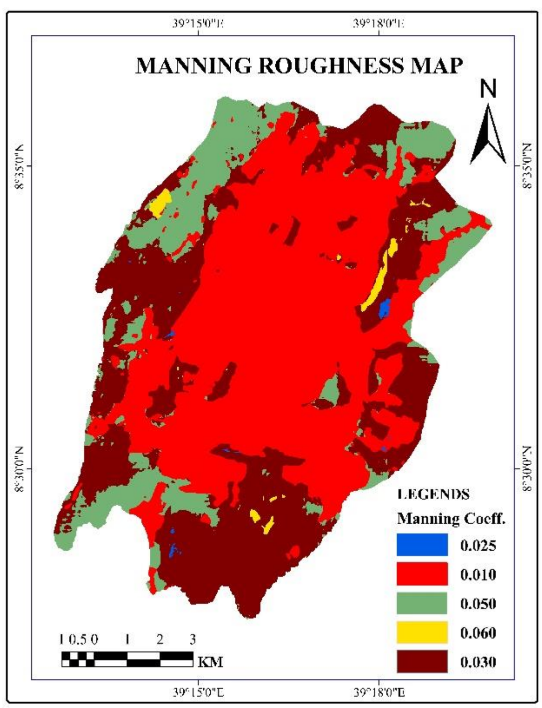

Figure 3.3. LULC-based Manning roughness coefficients map

3.7.Super-Fast Flood Model

In this study, the method developed by van den Bout et al. (2023) was used to simulate the flood inundation depth of Adama City. Hence, steady-state flow height was estimated first by running a minimal steady-state solver to find a stable directional velocity field, and flow accumulation was carried out on the velocity field to solve for steady-state discharge. Finally, the computed discharge was inverted to estimate the steady-state flow height. The compensation scheme was run for the partial steady-state flow of the event, and pressure-based inundation was compensated through an adaptive diffusive-wave solver.

The SFF was run to compute flood inundation depths for three cases: first for the RF event of April 18, 2000, and future scenarios using the RFI of a 50-year recurring period for both the IMD and ERA methods. To run the simulation, a DEM of 12.5m × 12.5m was loaded into SFFM, and after noise filtering and hydro-correction were employed for DEM quality purposes, a Sentinel-2 LULC of 2022 at 10m × 10m resolution, and Manning values for each land use type were assigned. A single RFI was used for the entire catchment for each simulation, as shown in Table 3.5. The infiltration map was again downloaded automatically from soilgrids.org, and the infiltration rate was assigned based on estimated infiltration rates with (Saxton & Rawls, 2006) Pedo-transfer functions as shown in Figure 3.4. The chosen soil grid depth was 5-15 cm. Finally, the model was run for each RF case using high solver accuracy.

Table 3.5. Rainfall input data for SFFM

			Scenarios
RF event	RFI (mm/hr)	Duration (hr)	Return period (year)
April 18, 2000	35.5	0.5	-
IMD based	55.6	0.5	50
ERA based	78	0.5	50

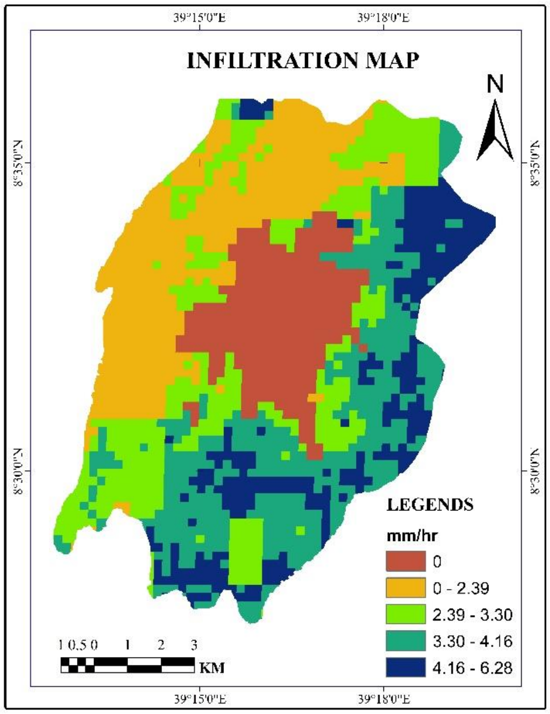

Figure 3.4. Soil texture-based infiltration rates map

3.8.Validation of the Flood Hazard Map

Model validation is the process of appropriately testing a model's outputs against different observed datasets of the real world to see how well they quantitatively and qualitatively match reality. Many researchers employ a variety of models to evaluate flood vulnerability around the globe, but it is crucial to examine the model's output to make sure it accurately reflects the actual ground conditions or observed data (Hagos et al., 2022d). Adama City had no stream flow gauge station, which was crucial for the calibration and validation of this study's output. Due to the lack of a discharge gauge station and limited satellite data, a field investigation, a local resident interview, and comparing the output of both models were undertaken for validation purposes.

3.9.Conceptual Framework of the research

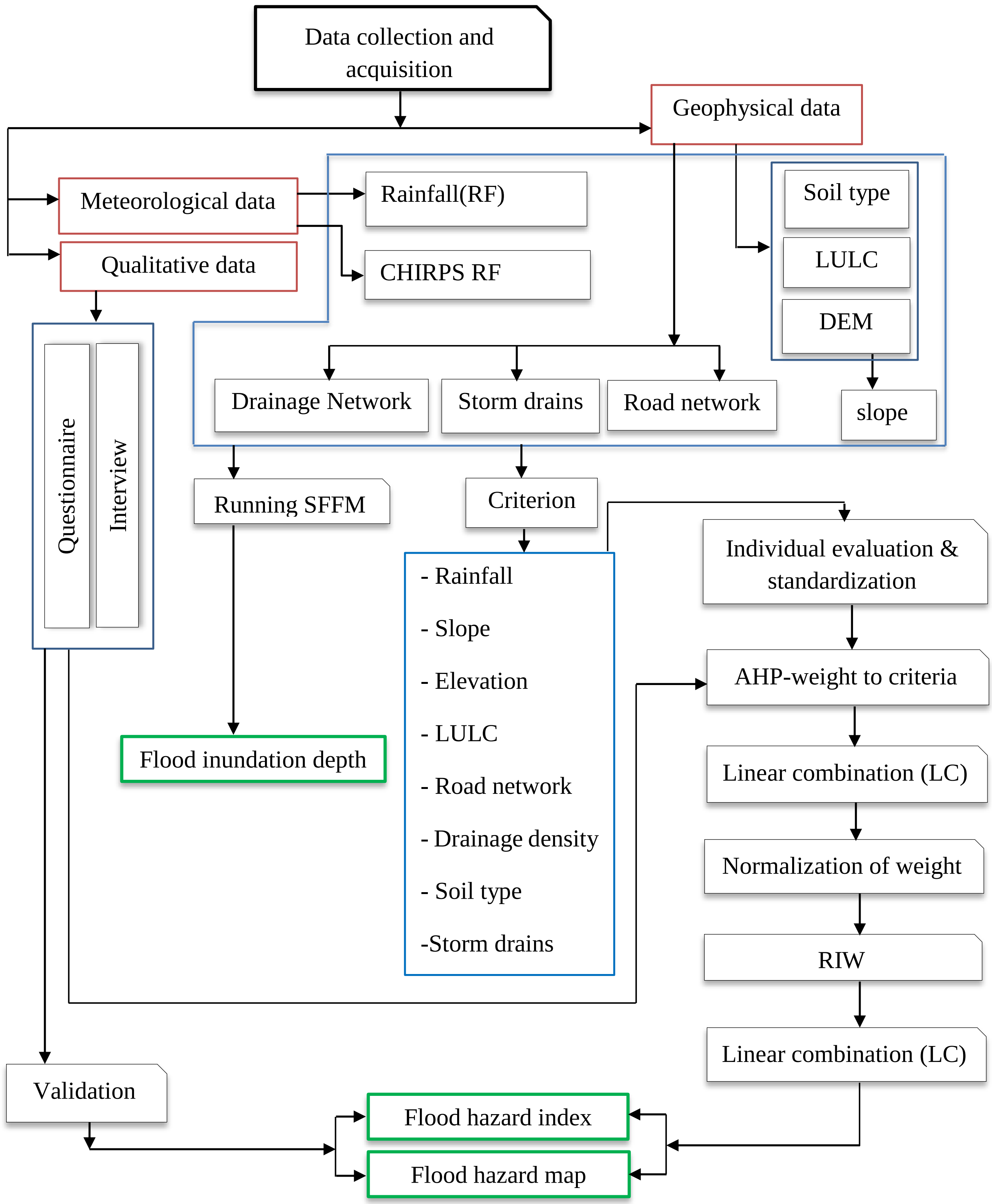

Figure 3.5. Flow chart for methodology

4. RESULT AND DISCUSSION

4.1. Flood Causing Factors

The selection of Adama City flood causing factors was conducted based on literature reports by considering the specific context of flooding in the city. From the analysis, eight critical flood causative factors were identified as crucial determinants of flood hazard in the area. These factors include elevation, drainage density, land use land cover (LULC), road network, slope, storm drains, rainfall, and soil type. Through analyzing each factor individually and overlay analysis the comprehensive weighted flood hazard map was generated to aid in understanding and managing the potential flood-prone areas within the city.

The selection of these specific flood causative factors highlights the multidimensional nature of flood hazard in Adama City. Elevation plays a crucial role in determining the vulnerability of areas to flooding, as low-lying regions are more susceptible to inundation during heavy rainfall events. Drainage density and the presence of storm drains influence the water flow patterns, affecting the severity and extent of flooding. Land use land cover (LULC) and road networks impact the permeability of the terrain, affecting how water is absorbed or redirected during floods, storm drains have impacts on draining excess water away from streets and urban areas during heavy rainfall events. Additionally, factors like slope, rainfall, and soil type contribute to the overall susceptibility of an area to flooding

4.1.1. Elevation

The analysis of Adama City's elevation revealed distinct variations across different regions. The north-west part of the city exhibited the highest elevation, ranging between 1871 to 1970 meters above mean sea level (a.m.s.l). On the contrary, the south-west and Eastern parts of the city had considerably lower elevations, ranging from 1475 to 1574 meters (a.m.s.l). The central part of the city had also a relatively lower elevation compared to the northwest, but higher than the south-western and Eastern areas, as depicted in Figure 4.1(a). These elevation patterns are crucial in understanding the city's topography and can significantly impact its susceptibility to flooding, with lower-lying areas being more prone to inundation during heavy rainfall events. The reclassified elevation map was generated based on scale influences as shown in Figure 4.1(b).

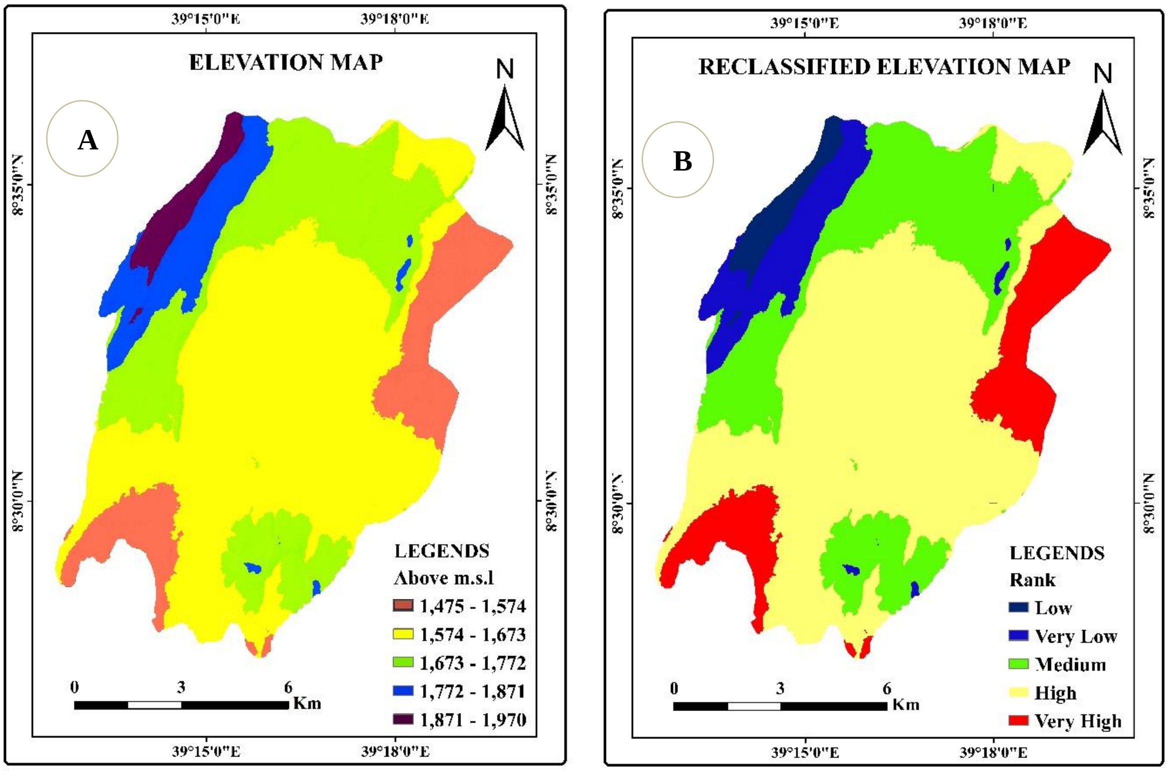

Figure 4.1. Adama City elevation and its weighted map

4.1.2. Drainage density

The drainage map of Adama City indicates a concerning situation, with a significant portion of the city exhibiting a poor drainage network, particularly in the Low-lying areas like Migira and Gara Lugo Kebeles as depicted in Figure 4.2(a). This poor drainage network made an area susceptible to flooding. The reclassified drainage density map was generated based on scale influences as shown in Figure 4.2(b).

4.1.3. Land use land cover

The land use land cover (LULC) of Adama City unveiled the prominent features that shape its landscape. The major LULC categories identified in the city included built-up areas, bare ground, cultivated crops, dense vegetation, and range land, as visually depicted in Figure 4.3(a). The built-up areas indicated the extent of urban development and infrastructure, while the presence of bare ground demonstrated open spaces and undeveloped lands. Cultivated crops reflected the agricultural activities within the city, and dense vegetation regions indicated green spaces and natural habitats. The range land category showcased areas consisting of natural grasses and shrubs. The reclassified LULC map was generated based on scale influences as shown in Figure 4.3(b).

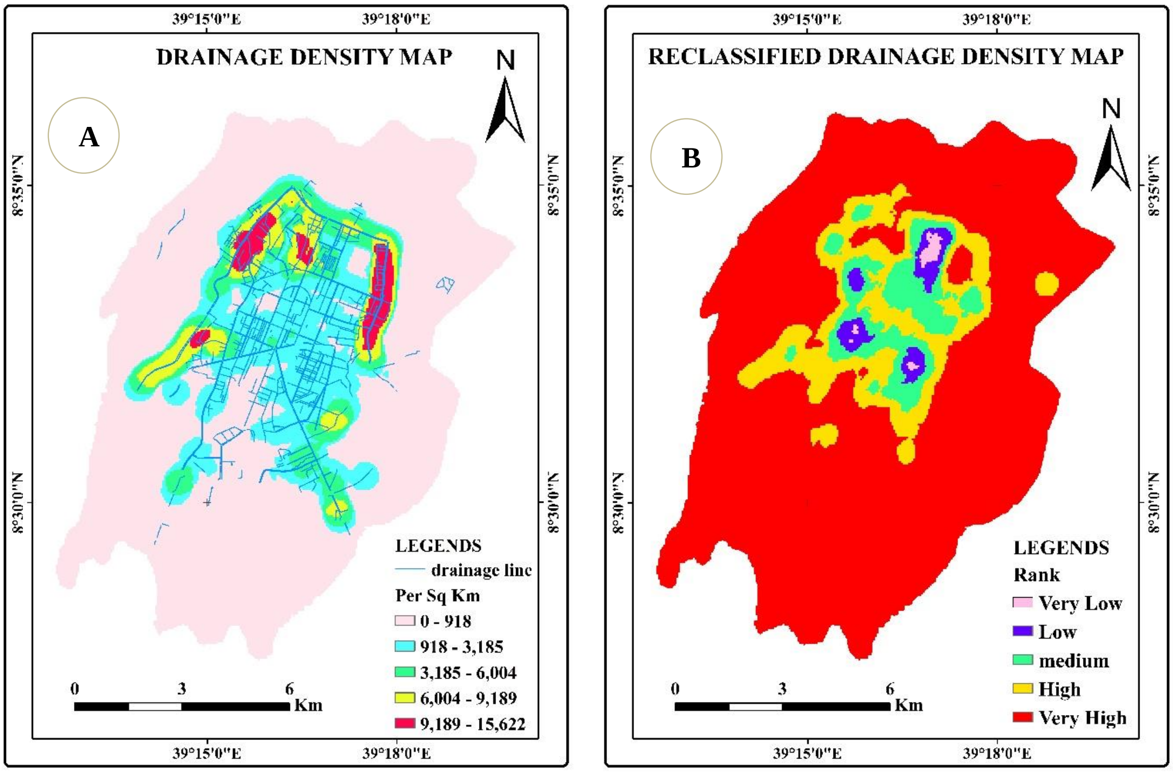

Figure 4.2. Drainage density and its weighted map

4.1.4. Road network

The analysis of the road network in the City revealed a significant concentration of roads in the central parts, characterized by dense urbanization. However, this dense road infrastructure posed challenges related to flooding, primarily due to the impervious nature of the road surfaces, which hindered water infiltration and natural drainage patterns. Consequently, this alteration of the natural drainage patterns exacerbated the city's susceptibility to flooding during heavy rainfall events. Figure 4.4(a) illustrates the detailed road network of the City. The reclassified road network map was generated based on the scale of influences as shown in Figure 4.4(b).

4.1.5. Slope

The slope analysis of Adama City showed a diverse topography with slopes ranging from 0 to 85 percent. However, the majority of the city's terrain exhibited a relatively flat slope, ranging from 0% to 17%, as depicted in Figure 4.5(a). This flat slope was prevalent across various parts of the city. The city's susceptibility to flooding is exacerbated by its natural boundary, consisting of the steepest slopes surrounding the area. This topographical feature necessitated efficient runoff of water towards the central parts of the city during heavy rainfall events, leading to potential inundation in low-lying regions within the city. The reclassified slope map was generated based on a scale of influences as shown in Figure 4.5(b).

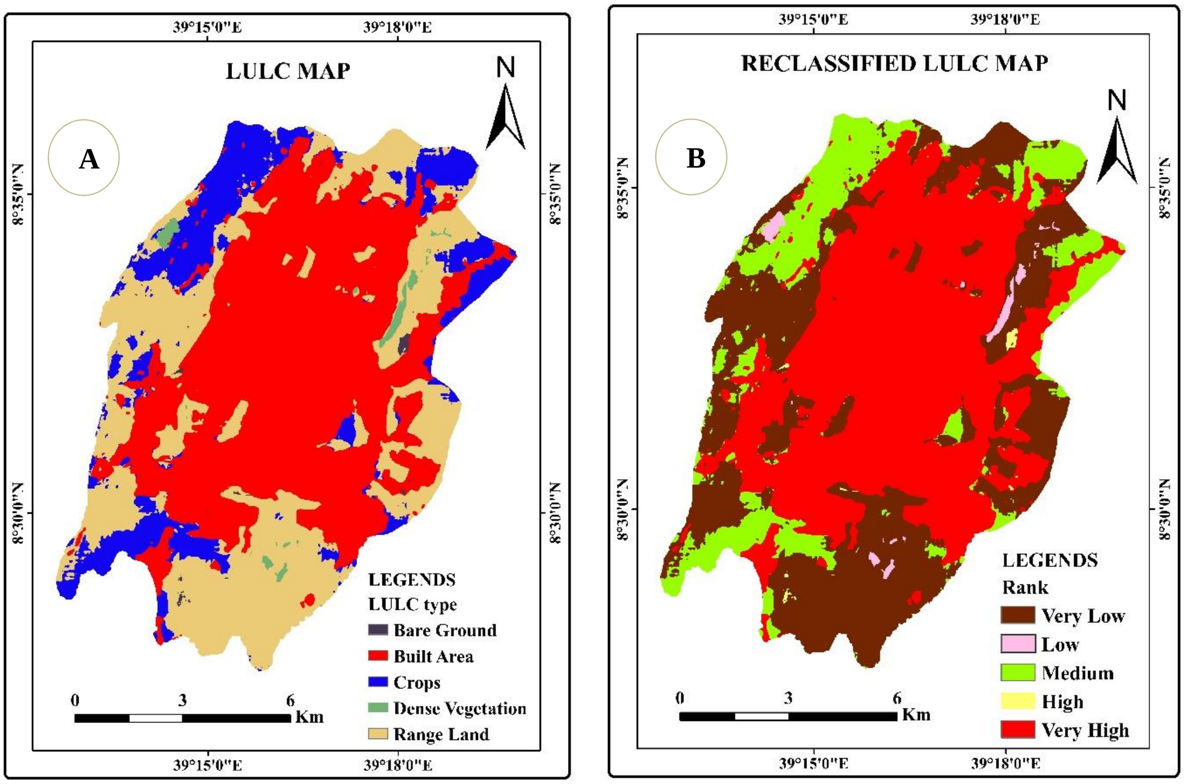

Figure 4.3. Land use land cover and its weighted map

4.1.6. Storm drains

The analysis of storm drain distribution highlighted a concerning pattern, and showed a poor coverage over flood-prone areas of the city. Figure 4.6(a) illustrates the inadequacies of storm drain distributions, which can significantly exacerbate the city's vulnerability to flooding during heavy rainfall events. The lack of sufficient storm drains infrastructure in flood-prone areas of the city has led to water accumulation and increased flood risks. The reclassified storm drains map was generated based on scale influences as shown in Figure 4.6(b).

4.1.7. Rainfall

The CHIRPS spatial average annual rainfall in southern parts of the city ranged from 659 to 787 mm/year, indicating a relatively low compared to other areas. Conversely, the North and northwest parts experienced higher precipitation, with average annual rainfall ranging from 819 to 850 mm/year. The Eastern part of the city fell in between, with rainfall varying from 787 to 819 mm/year. Figure 4.7(a) depicts the average annual rainfall distributions of Adama city. The reclassified rainfall map was generated based on a scale of influences as shown in Figure 4.7(b).

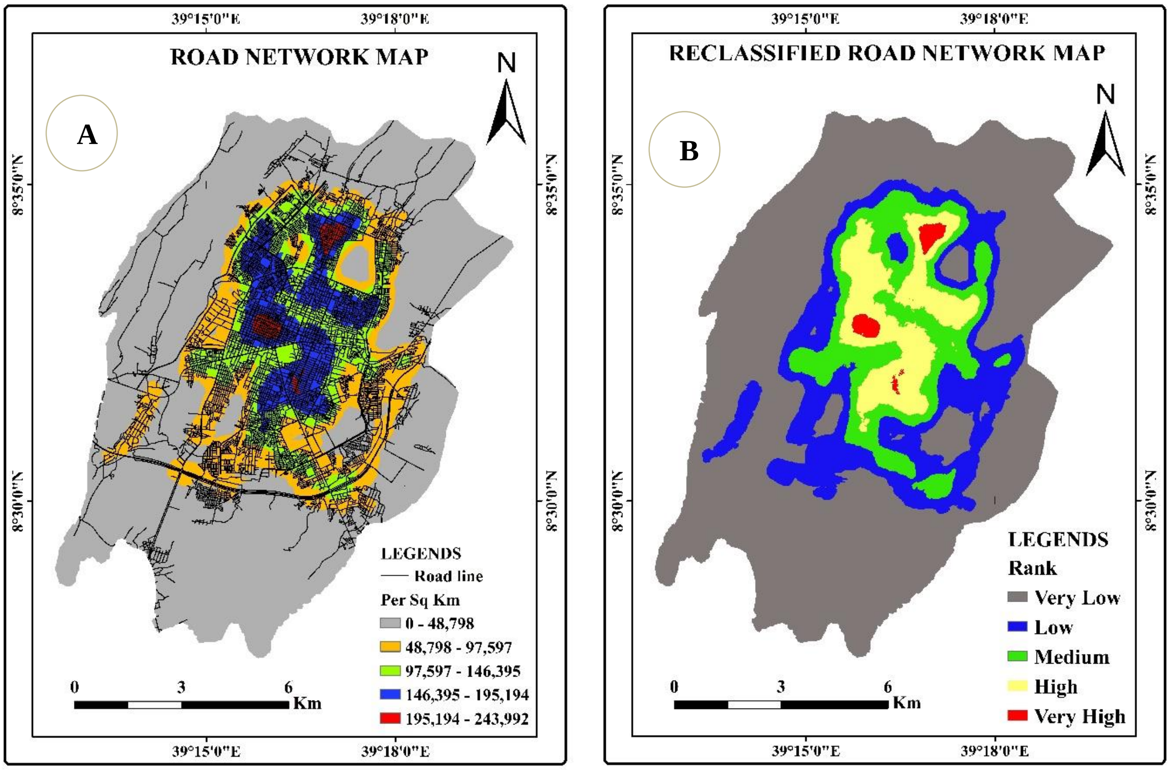

Figure 4.4. Road network and its density's weight map

4.1.8. Soil type

The soil textures were categorized as clay loam, loam, sandy, sandy loam, and silty clay, as presented in Figure 4.8(a). The northern parts were characterized mainly characterized by sandy and silty soil texture. Whereas, the southern border exhibited loam soil and the eastern parts were characterized by clay and sandy loam. The reclassified soil texture map was generated based on scale influences as shown in Figure 4.8(b).

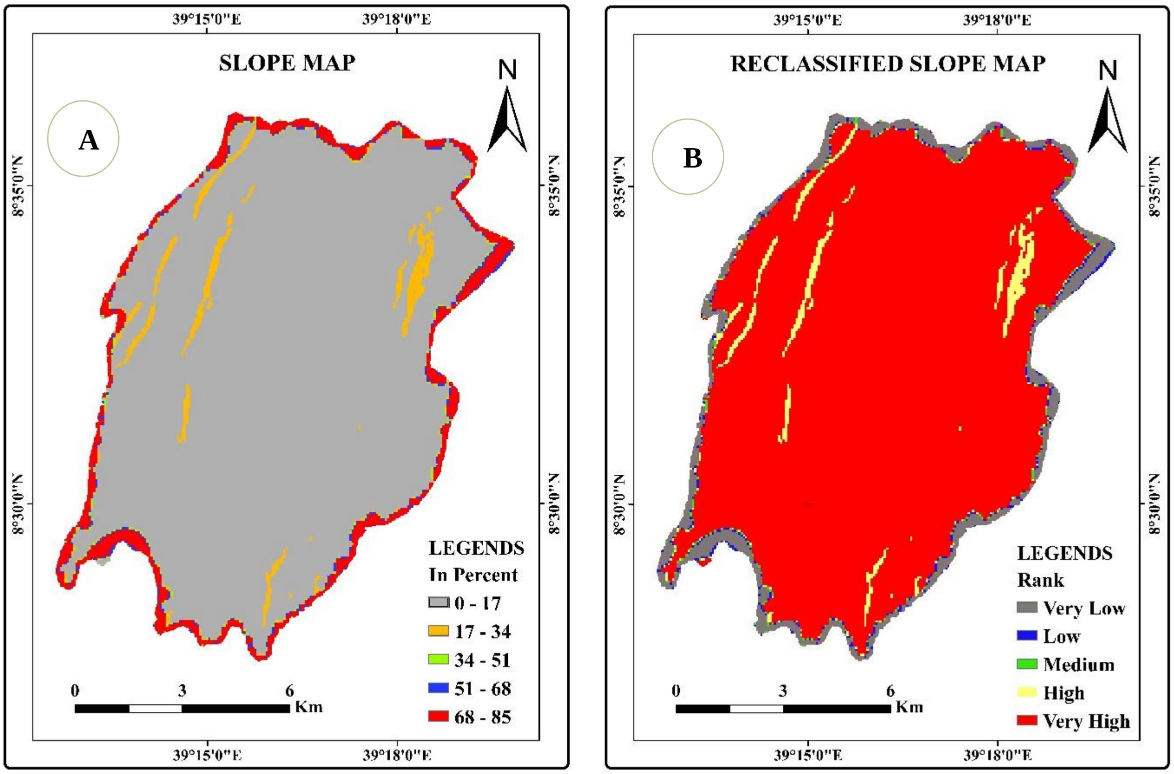

Figure 4.5. Adama city slope and its weighted map

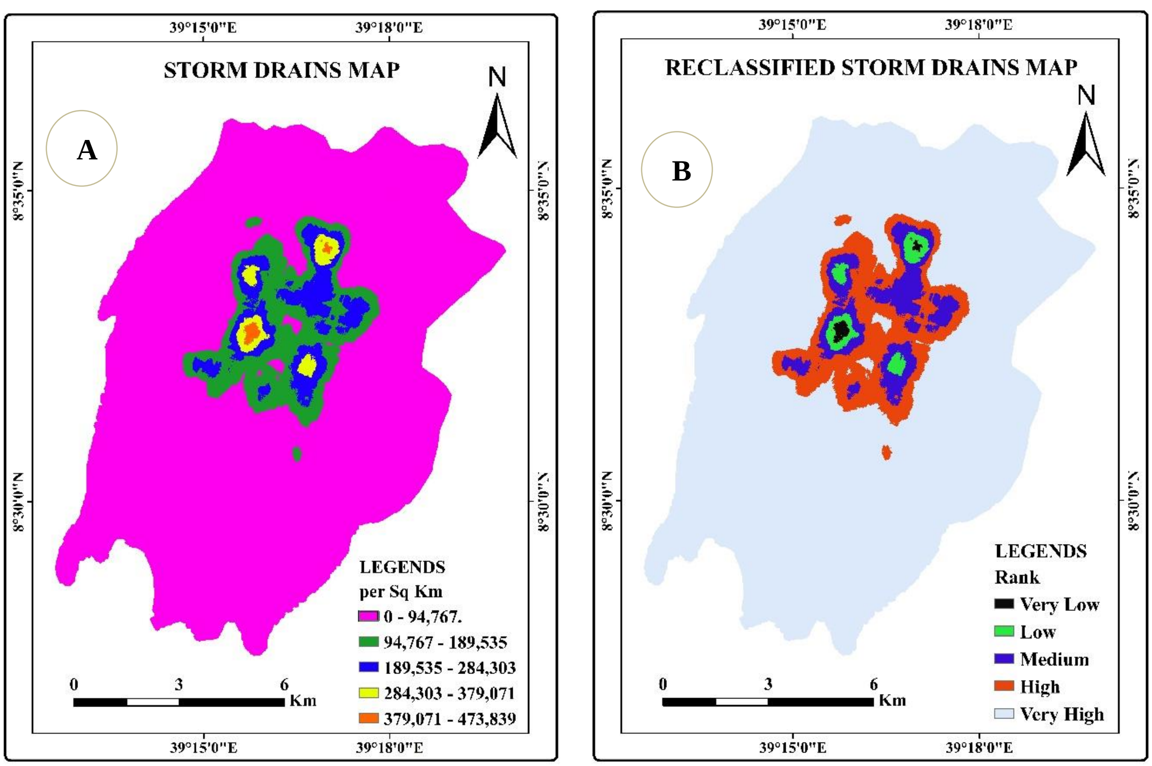

Figure 4.6. Storm drains and its weighted map

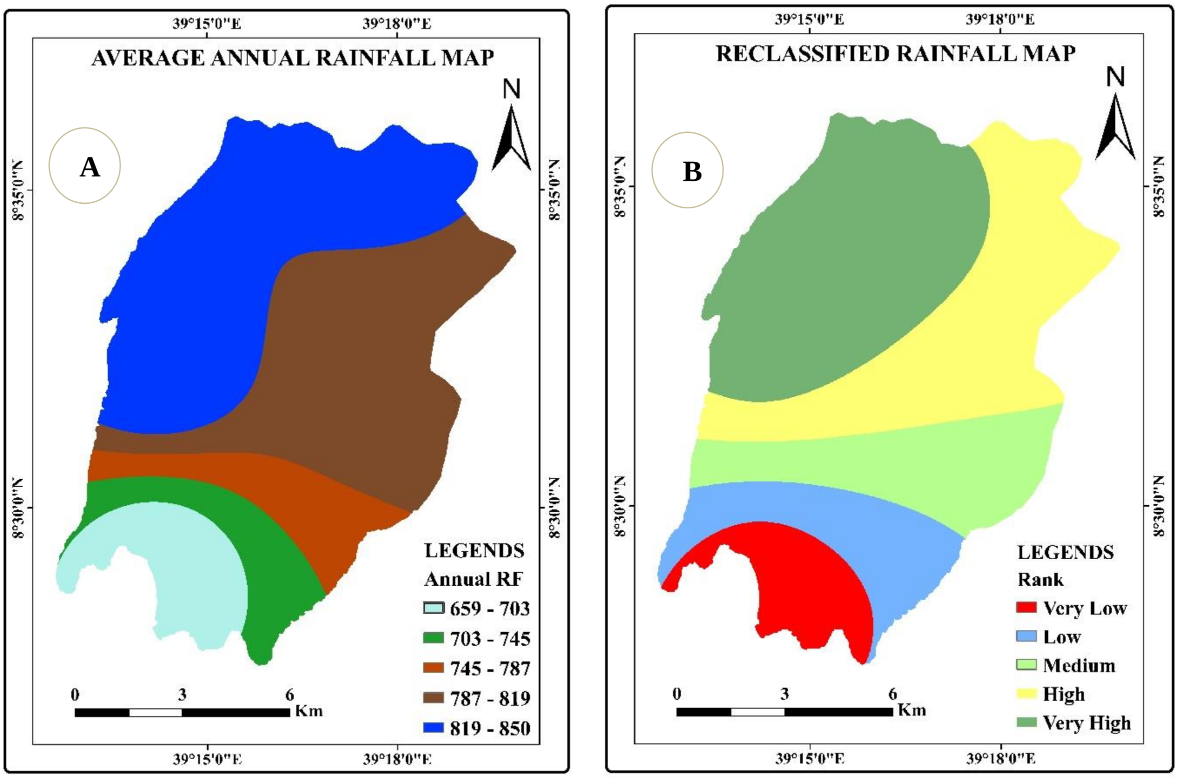

Figure 4.7. Average annual rainfall and its weighted map

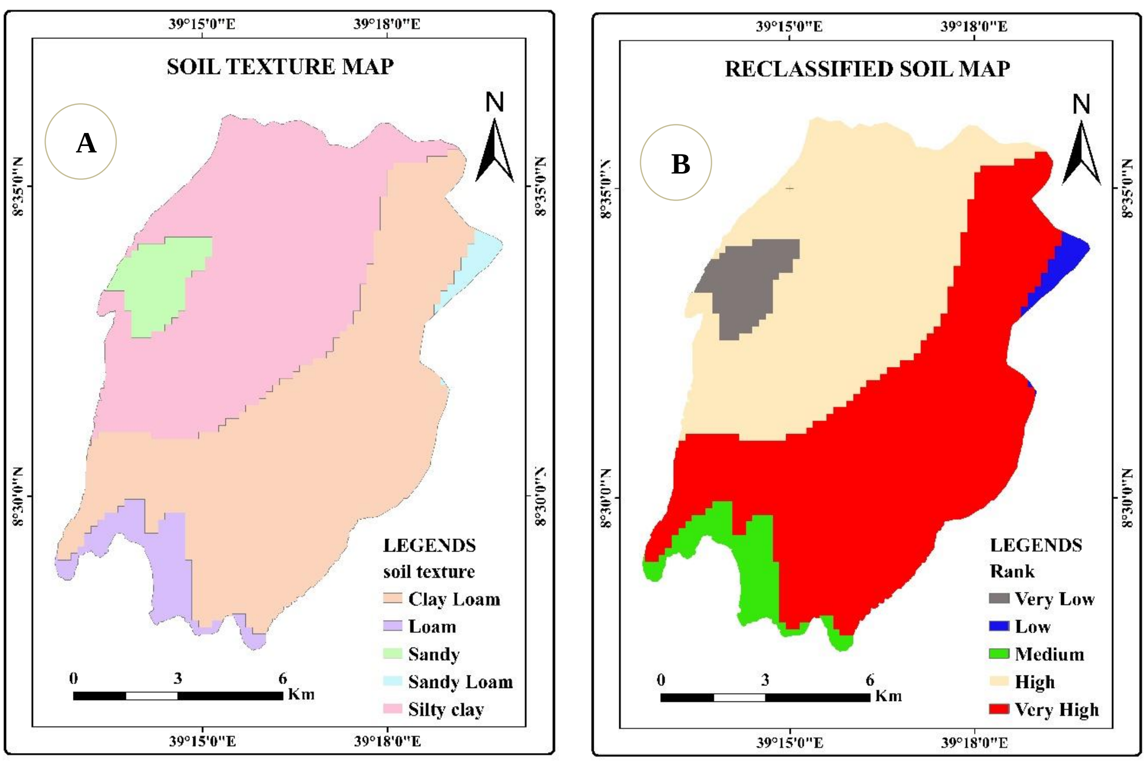

Figure 4.8. Soil texture and its weighted map

4.2.Pair-wise Comparison

The flood generating factors employed in this study were prioritized and given a relative weight based on 15 responded questionaries' using the AHP pairwise comparison matrix as shown in Table 4.1. The normalized pair-wise comparison matrix was computed as shown in Appendix Table 1. and the consistency of the pair-wise matrix was checked as depicted in Appendix Table 2. The consistency ratio of the AHP pair-wise matrix was 0.04. The AHP pair-wise comparison matrix analysis adopted in this matrix was consistent according to Saaty (2008), because the obtained value of CR was less than 10%.

Table 4.1. AHP pair-wise comparison matrix

Factors	Elevation	DD	LULC	RN	Slope	SD	Rainfall	Soil type
Elevation	1	1	3	4	2	5	2	6
DD	1	1	3	4	2	4	2	5
LULC	1/3	1/3	1	3	3	4	1	5
RN	1/4	1/4	1/3	1	3	3	1/3	5
Slope	1/2	1/2	1/3	1/3	1	3	2	5
SD	1/5	1/4	1/4	1/3	1/3	1	1/3	5
Rainfall	1/2	1/2	1	3	1/2	3	1	1/3
Soil type	1/6	1/5	1/5	1/5	1/5	1/5	3	1

Figure 4.9 shows the obtained relative weight of flood causative factors using the AHP pair-wise comparison matrix. Flood susceptibility in Adama City was influenced by a complex interplay of various factors, each exerting its distinct impact as shown in Figure 4.9. Elevation, contributing 22% to flood causes, plays a significant role in determining the city's vulnerability to flooding. Hence, Migira, Gara Lugo, and Irrecha kebeles was lower-lying areas and highly susceptible to inundation. Drainage density, with a weightage of 21%, influences the efficiency of conveying runoff water. Unfortunately, the low-lying areas around Migira, Gara Lugo, and Irrecha did not have a sufficient drainage network, affecting the areas to manage excess water during heavy rainfall. Land use and land cover, accounting for 14%, directly influence the permeability of surfaces, altering the rate at which rainwater infiltrates into the ground and exacerbating surface runoff.

Slope, contributing 12%, determines the flow velocity and direction. The Adama city slope showed the flow direction was appearing mainly towards Migira, Gara Lugo, and Irrecha kebele's. The Rainfall patterns, 11%, was a pivotal factor in flood causes, as intense precipitation events can overwhelm drainage systems. The road network, comprising 9%, affects floodwater flow paths, potentially obstructing natural drainage routes, and infiltration into the ground. The effectiveness of storm drains, at 6%, was crucial in channeling excess water away from urban areas but, storm drains distribution was very poor mainly around Migira and Irrecha kebeles again. Lastly, soil type, at 5%, determines the soil's capacity to absorb water, influencing the potential for surface runoff.

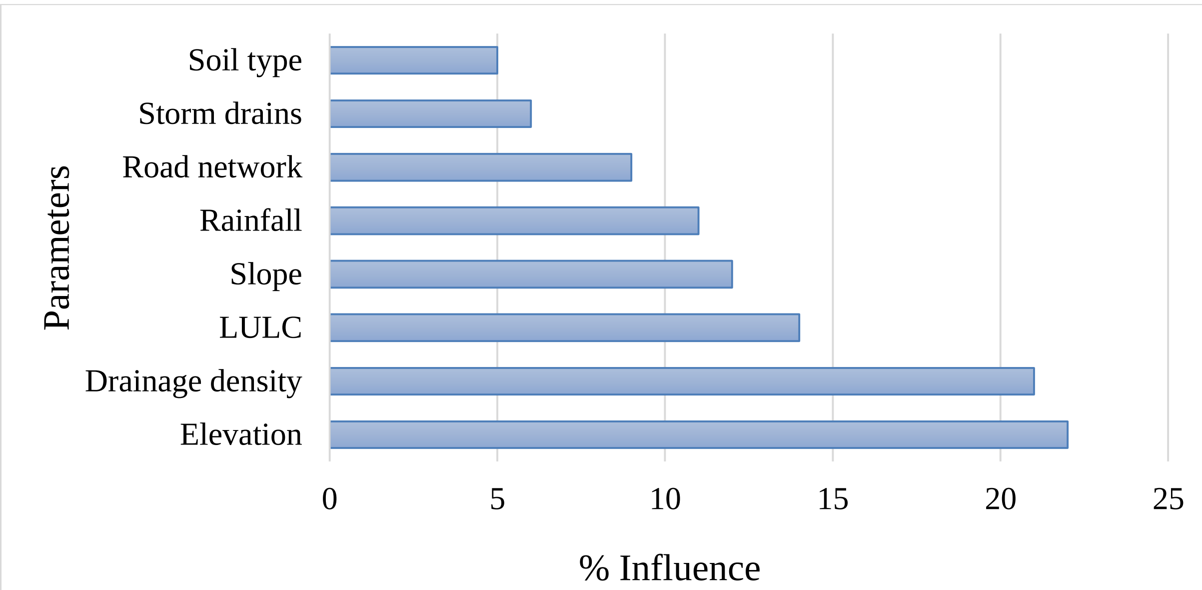

Figure 4.9. percent influence of flood causing factors in the city

4.3.Flood Hazard Map

The flood hazard map of the city was generated through overlay analysis of the undertaken flood causing factors in the city. Figure 4.10 shows the potential flood-vulnerable areas and their hazard index.

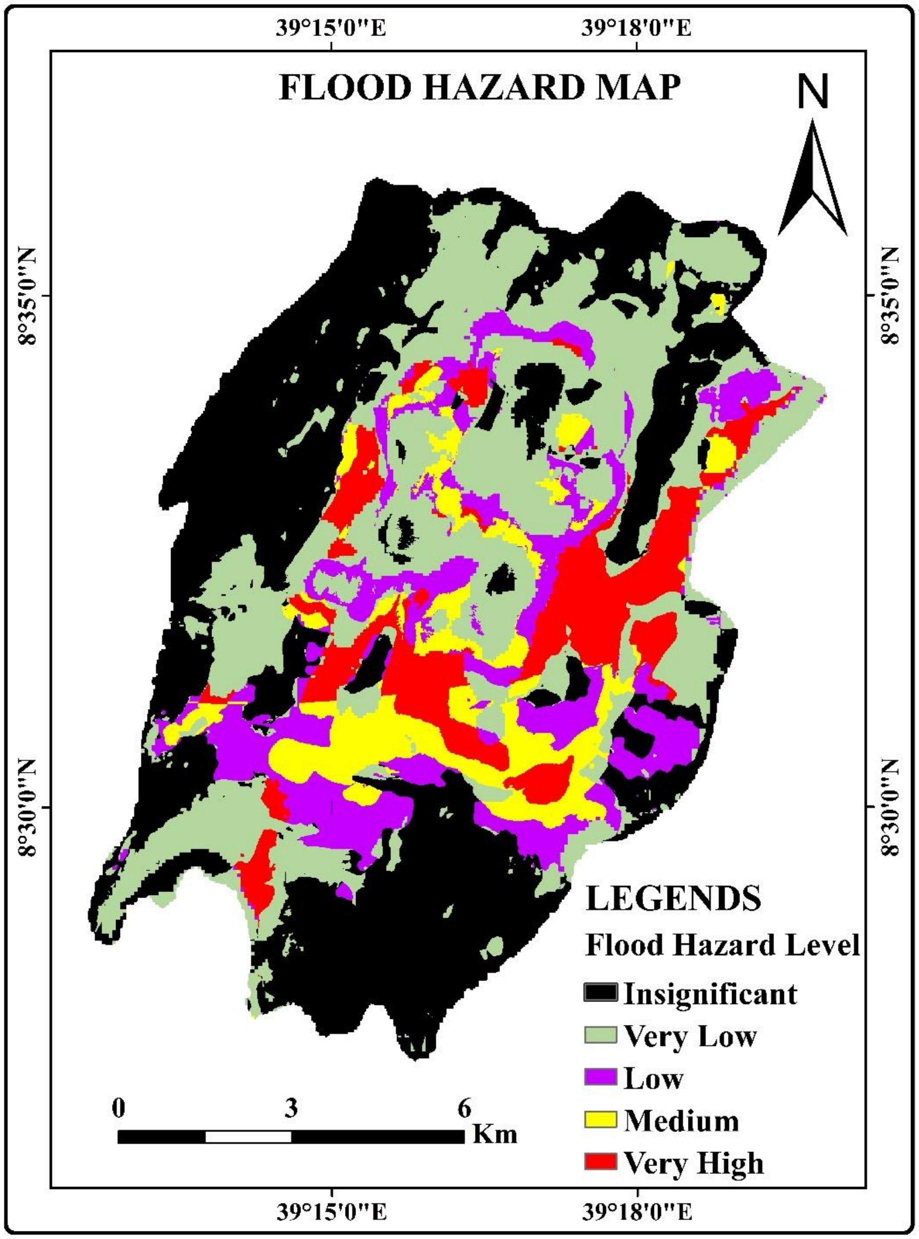

Figure 4.10. Adama city flood hazard map

The generated flood hazard map was shows distinctive hazard levels across various areas of the city. The North-Western, Northern, and South-Eastern regions exhibit minimal and insignificant flood hazard, owing to their elevated terrain. Conversely, the central, south-western, and middle eastern sections demonstrate varying degrees of flood susceptibility, attributed to their lower elevation, inadequate drainage systems, and extensive urban development. Notably, Migira (02), Gara Lugo (03), and Irrecha (09) Kebeles emerge as significant areas within the high to medium flood hazard level. Furthermore, the flood hazard assessment showed some specific areas within Irrecha Kebele, namely around Afomia Guest House, Principal's Health and Business Administration College, southern parts of Haile Resort, and around Oromia Sp. boarding and Adama Mosque, as being particularly susceptible to high flood hazard level, as indicated in Figures 4.11 (A and B) and Figure 4.12.

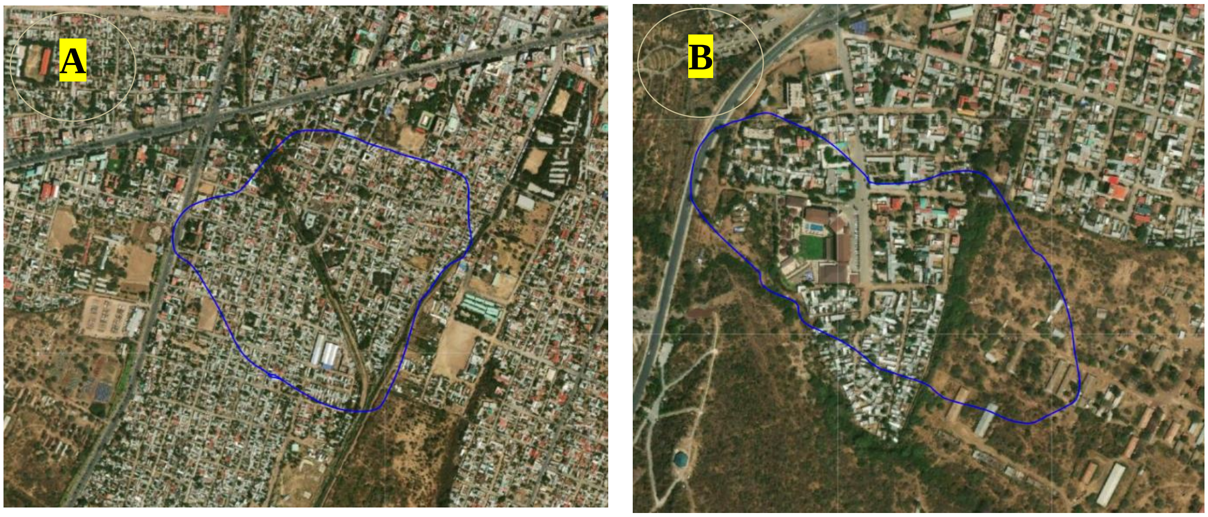

Figure 4.11. Around Afomia guest house (A) and around Haile resort (B)

Figure 4.12. Around Oromia Sp. boarding, and Adama mosque

Again, the Western parts of Gada Street (around MOENCO and Ethio-Engineering group Adama agricultural machinery manufacturing industry) are highly characterized by industries are under high flood hazard level as shown in Figure 4.13.

Figure 4.13. Western parts of Gada street

Migira kebele' s which is characterized by a poor drainage network; and low elevation was subjected to a high flood hazard according to this study. Figure 4.14 shows flood-susceptible areas around Migira Pond and St. John Church.

Figure 4.14. Around Migira Pond and St. John Church

The areas encompassing Gara Lugo Kebele, in proximity to the Tikur Abay bus station, and along the Ebisa Adugna road were found to be at a high susceptibility to flooding as shown in Figure 4.15. This high flood hazard can be attributed to deficient drainage density, a low elevation profile, and inadequate management of the existing drainage infrastructure.

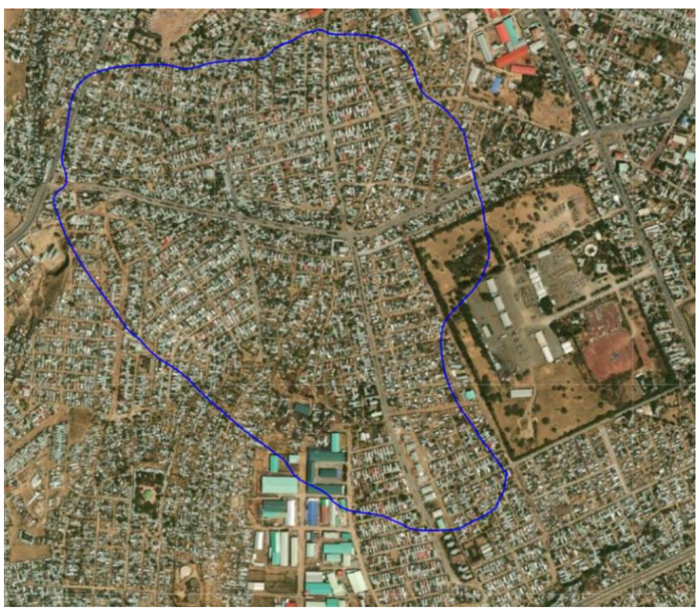

Figure 4.15. Around Tikur Abay bus station and alongside Ebisa Adugna road

4.4.Intensity Duration Frequency (IDF) Curve

The storm drainage system of Adama City showed inadequacies, mainly in flood-prone areas, as obtained from overlay analysis. The analysis of the elevation and slope of the city exhibited the lowest and flattest slopes, respectively. Thus, to minimize the risk of flooding, it is necessary to provide a sufficient and efficient drainage system in the city. The IDF curve was developed for 2, 10, 25, 50, 75, and 100 years, as shown in Figure 4.16. Hence, the IDF curve contains crucial insights into RF patterns, their associated intensity, storm duration, and frequency. By examining this data, city planners can identify the maximum expected rainfall intensity for various durations and return periods. This understanding helps in choosing suitable capacities for drainage systems and design parameters, ensuring the network can efficiently manage runoff and prevent flooding in different storm scenarios.

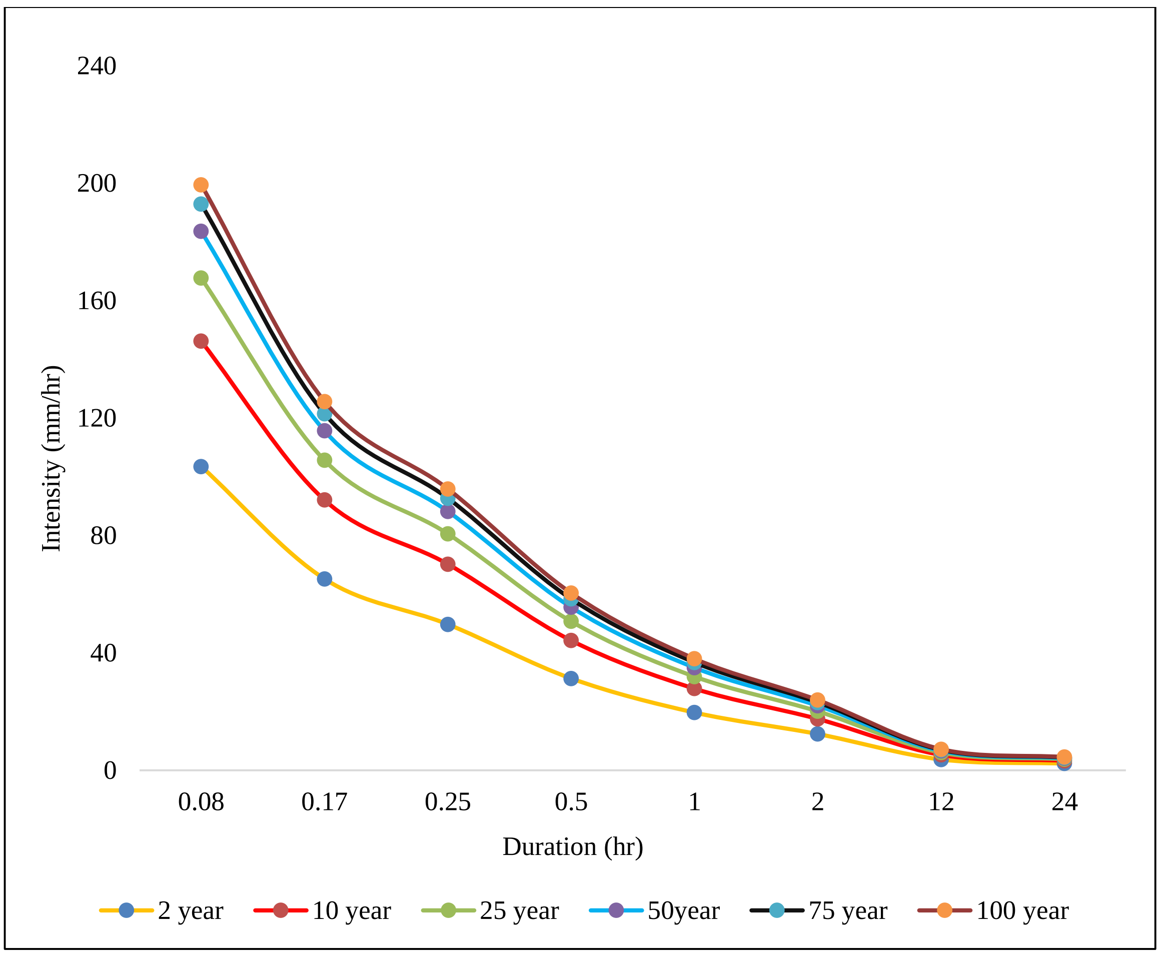

Figure 4.16. IDF Curve for IMD methods short duration RF

4.5.Flood Inundation Depth

The superfast flood (SFF) model was first simulated based on the rainfall event of April 18, 2000. The SFF model uses a single rainfall intensity for a specified storm duration. Hence, from the IMD method of 35.5 mm/hr rainfall intensity for 0.5 hr duration was used for simulation as shown in Figure 4.17. The simulation of SFF inundation depth shows the maximum flow depth of 0.8m to 1.8m meter was appeared in Migira kebele around Migira pond and Irrecha kebele around Afomia hotel, while minimum to high flow depth of 0.02m to 0.8m flash flood appeared in Gara Lugo kebele around Ebisa Adugna road and Migira kebele around St. John Church.

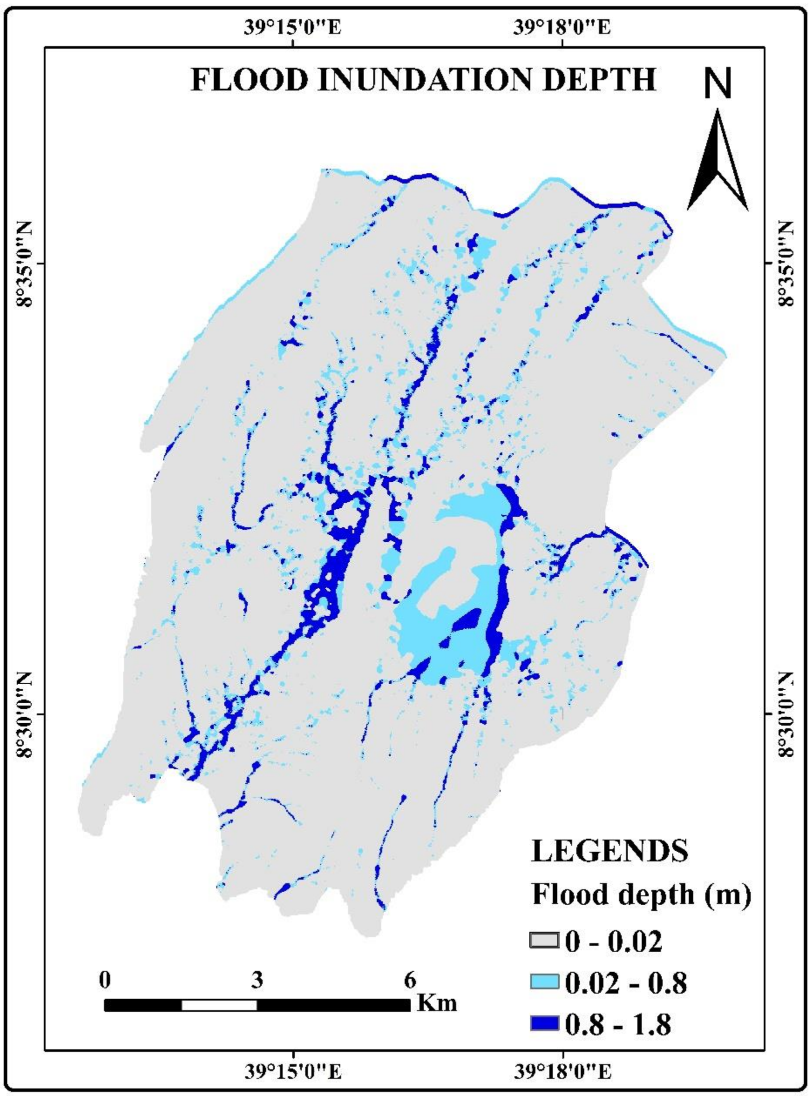

Figure 4.17. Flood inundation depth for IDM of 35.5 mm/hr

4.6.Flood Inundation Depth for a 50 Year Return Period

The flood inundation depth for the 50 year return period was simulated based on the Indian Meteorological Department (IMD) method of short-duration rainfall and Ethiopian Roads Authority (ERA) short-duration rainfall for a 50-year recurring period. For the IMD method, a rainfall intensity of 55.6mm/hr for a storm duration of 0.5 hours was selected after RF frequency analysis using HEC-SSP. As for the Ethiopian Road Authority (ERA) method, a 50-year recurring period of 78mm/hr rainfall intensity (RFI) for a 0.5-hour storm duration was adopted from the study conducted by (Aychiluhim, 2016). In the first scenario of IMD, the simulation result showed a maximum flood inundation of 1.95m around Migira Pond and 0.5m around Awash Hotel, as depicted in Figure 4.18. In the second scenario for the ERA method, the flood inundation depth simulation exhibited a maximum flood depth of 2.3m, mostly around Migira Pond and 0.9m around Awash Hotel as illustrated in Figure 4.19.

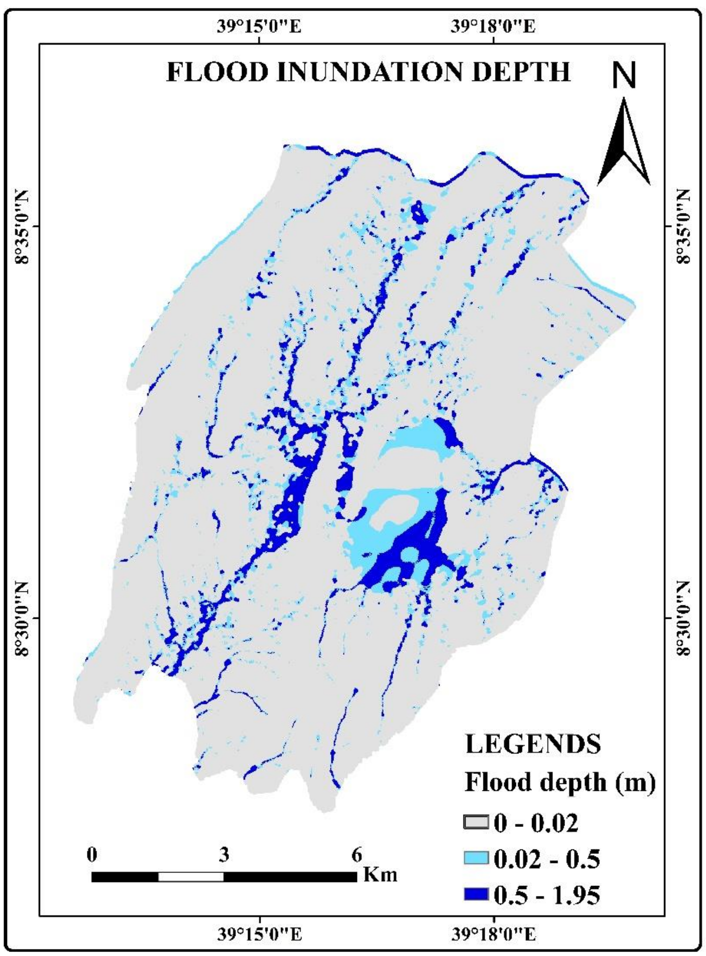

Figure 4.18. Flood inundation depth for IMD 50-year RP scenario

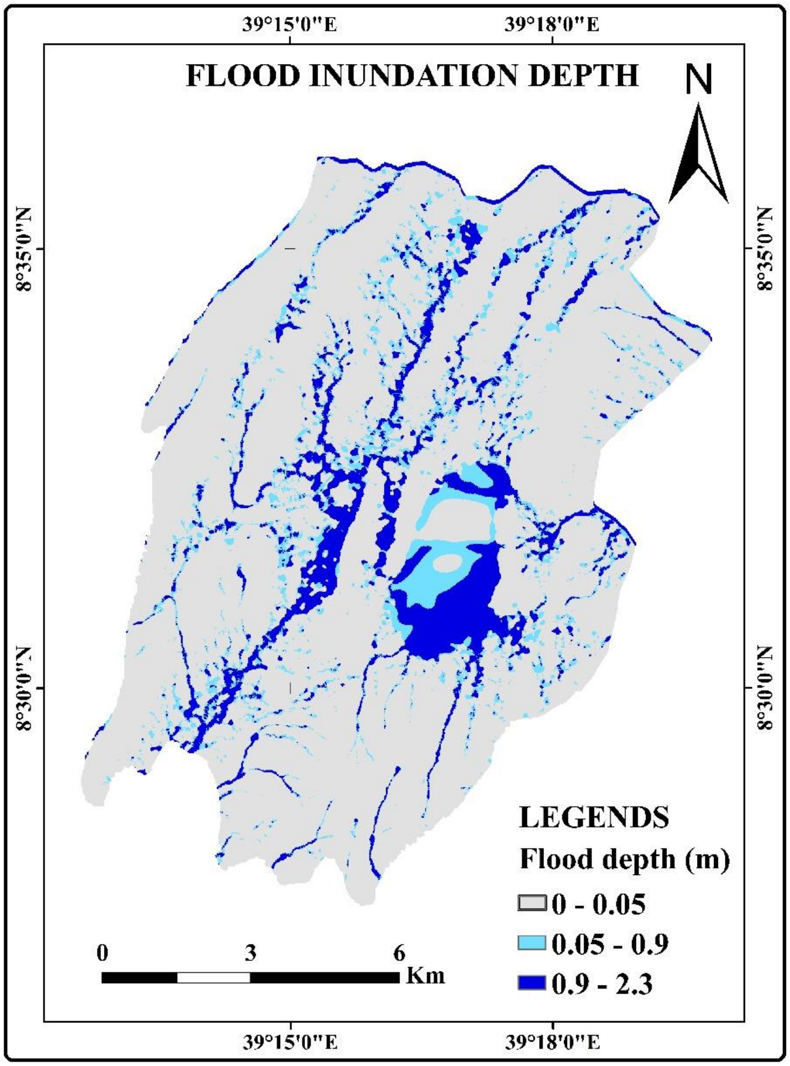

Figure 4.19. Flood inundation depth for ERA 50-year RP scenario

4.7.Model validation

The validation process of the simulated flow depth and flood extent results in Adama City faced unique challenges due to the absence of stream flow gauge stations and limited satellite products capturing water extent. Without stream flow gauge stations, the calibration and validation of simulated flow depth became a complex task. Additionally, the satellite products only provided information about the water extent in Migira pond, possibly influenced by factors such as building density and tree cover. Consequently, alternative methods were sought to validate the results. The chosen approach involved conducting interviews with local residents from flood-prone areas and comparing the outcomes of two different models. Despite the limitations, this method provided valuable insights into the accuracy of the simulated results.

To overcome the lack of stream flow gauge stations and limited satellite data, a practical validation strategy was employed, centering on interviews with residents from flood-susceptible areas. Through interviews with ten individuals residing in various vulnerable locations, including Migira, Gara Lugo, and Irrecha Kebeles, crucial information regarding historical flood events in 2000, 2006, and 2016 was gathered. Notably, the residents confirmed property damages in these Kebeles during the mentioned flood years. Specific inundation areas were identified, such as around Gara Lugo (03) Kebele near the police station, western parts of Gada street, the southeast of Migira bus station south-eastern parts of Haile resort. Based on the response of interviewees both AHP-GIS and SFFM models exhibited a good accuracy in delineating flooding extent. Moreover, field observations revealed inadequacies in drainage channels, particularly in Migira and the upper parts of the Irecha kebele catchment where natural gullies played a crucial role in channeling floodwaters. The field assessment also showed the blockage of storm drains by solid waste and soil accumulation, as documented in Appendix 6. These on-site findings corroborated the validity of the simulation results.

5. CONCLUSION AND RECOMMENDATIONS

5.1.Conclusion

Flooding is a natural hazard that affects human life and the ecosystem globally, causing catastrophic disasters. Most flood-induced socioeconomic losses are exacerbated by unabated urban development, population upsurges, unregulated municipal systems, and indiscriminate land use. Flooding is one of the most common natural disasters, often with disastrous consequences, affecting 170 million people worldwide each year. Even though a flood is a natural disaster, it can be managed by properly implementing different structural and non-structural techniques. Hence, assessing the flood vulnerability, mapping the risk zones, and simulating the flood inundation depth areas are some of the prevalent techniques used to minimize the risk of flooding these days.

In recent years, Adama City has been severely affected by flooding problems. For instance, the city has experienced significant losses as a result of the floods that occurred in 2000, 2008, 2009, and 2016. Periodic observations showed a substantial increase in the social, economic, and ecological damages caused by flooding. This is because the city does not have a comprehensive early warning system for managing flood risk. These issues clearly call for continual improvement in analysis, mitigation, and management.

This study employed the integrated multi-parametric AHP-GIS and super-fast flood models. AHP-GIS was used to generate a flood hazard map through overlay analysis of flood causative factors such as elevation, drainage density, land use, land cover, slope, road network, storm drains, soil map, and spatial average annual rainfall of the city. A super-fast flood model simulated flood inundation depth using DEM, spatial Manning coefficients, spatial infiltration, and short-duration rainfall intensity.

The generated flood hazard map that showed Irrecha, Migira, and some areas of Gara Lugo Kebeles were at high risk of flooding. These areas were characterized by a poor drainage network and storm drain distribution, as well as low elevation. The simulated flood inundation depth of 35.5 mm/hr demonstrated a maximum flood depth of 1.8m. In the 50-year return period flood simulation scenarios, the IMD method (55.6 mm/hr) showed a maximum flood depth of 1.95m, and the ERA method (78 mm/hr) showed a 1.95m maximum flood inundation depth. The maximum flood depth appeared in Migira and Irrecha Kebeles. The models were validated through interviews and field visits and showed good results based on local residents and experts interviews.

The responses of the interviewee showed there were flooding problems in the city, specifically in poor drainage networks and low-elevation areas such as Migira, Irrecha, and some parts of Gara Lugo Kebeles around the police station. Hence, the IDF curve was developed for 2, 10, 25, 50, 75, and 100-year return periods.

5.2.Recommendations

- The result of this study inferred that three kebeles were highly vulnerable to flooding. So, future studies can utilize the identified flood hazard index to assess how the community and its economy were affected during flood events.
- Again, future studies can utilize AHP-GIS fuzzification techniques to minimize the inconsistency of the pairwise comparison matrix.
- Policymakers and planners can use the results of this for flood protection, the planning and construction of any projects along the city's flood hazard area, and effective emergency responses for flood hazard areas in the city.
- Furthermore, the developed IDF curve will be helpful in planning and designing the drainage system of the city.
- The validation of simulated flow depth in Adama City faces a unique challenge due to the absence of a single stream flow gauge station in the city. Without stream flow gauge stations, the calibration and validation of simulated flow depth became complex tasks. Hence, the concerned body should install at least two gauging stations in the city.
- During the field visit, most of the storm drains and drainage lines were filled with solid waste and soil in Irrecha and Gara Lugo kebeles, so the Adama municipality should focus on frequently cleaning the drainage lines and storm drains.

REFERENCES

Achamyeleh, K. (2003). *Ethiopia: Integrated Flood Management*. 5.

Acharya, S. C., Nathan, R., Wang, Q. J., & Su, C.-H. (2022). Temporal disaggregation of daily rainfall measurements using regional reanalysis for hydrological applications. *Journal of Hydrology*, *610*, 127867. https://doi.org/10.1016/j.jhydrol.2022.127867

Aggarwal, S., Thakur, P., & Dadhwal, V. (2009). Remote sensing and GIS Applications in Flood Management. *Journal of Hydrological Research and Development, Theme Flood Management*, *24*, 145–158.

Agonafir, C., Lakhankar, T., Khanbilvardi, R., Krakauer, N., Radell, D., & Devineni, N. (2023). A review of recent advances in urban flood research. *Water Security*, *19*, 100141. https://doi.org/10.1016/j.wasec.2023.100141

Arcement, G. J. Jr., Schneider, V. R., & United States. Geological Survey (USGS). (1984). *Guide for Selecting Manning's Roughness Coefficients for Natural Channels and Flood Plains* (FHWA-TS-84-204). https://rosap.ntl.bts.gov/view/dot/68015

Ariff, H., Salit, M. S., Ismail, N., & Nukman, Y. (2008). Use of Analytical Hierarchy Process (AHP) for Selecting The Best Design Concept. *Jurnal Teknologi*, 1â€“18-1â€“18. https://doi.org/10.11113/jt.v49.188

Arya, A. K., & Singh, A. P. (2021). Multi criteria analysis for flood hazard mapping using GIS techniques: A case study of Ghaghara River basin in Uttar Pradesh, India. *Arabian Journal of Geosciences*, *14*(8), 656. https://doi.org/10.1007/s12517-021-06971-1

Atanaw, F., & Beyene, T. (2016, May 17). *IDF Equations for Similar Rainfall Regions in Ethiopia*. https://www.researchgate.net/publication/316455984_IDF_Equations_for_Similar_Rainfall_Regions_in_Ethiopia

Aychiluhim, M. (2016). *Adama Flood Problem –Flood Risk Mitigation Option for Boku Shenen Area* [Thesis, Addis Ababa University]. http://etd.aau.edu.et/handle/123456789/9845

Basumatary, V., & Sil, B. S. (2018). Generation of Rainfall Intensity-Duration-Frequency curves for the Barak River Basin. *Meteorology Hydrology and Water Management.*

Research and Operational Applications, *Vol. 6*, *Iss. 1*. https://doi.org/10.26491/mhwm/79175

Beyene, T. D., Moges, M. A., & Tilahun, S. A. (2019). Development of Rainfall Disaggregation Model in the Awash River Basin, Ethiopia. In F. A. Zimale, T. Enku Nigussie, & S. W. Fanta (Eds.), *Advances of Science and Technology* (Vol. 274, pp. 50–64). Springer International Publishing. https://doi.org/10.1007/978-3-030-15357-1_4

Bibi, T. (2023). Derivation of short-term design rainfall intensity from daily rainfall data for urban drainage design using empirical equations in Robe Town, Ethiopia. *Journal of Hydrology*, *7*, 63. https://doi.org/10.15406/ijh.2023.07.00340

Bojovic, N., & Milenkovic, M. (2008). The best rail fleet mix problem. *Operational Research*, *8*(1), 77–87. https://doi.org/10.1007/s12351-008-0012-8

Borga, M., Comiti, F., Ruin, I., & Marra, F. (2019). Forensic analysis of flash flood response. *WIREs Water*, *6*(2). https://doi.org/10.1002/wat2.1338

Bout, B. van den. (2022). *Super-fast flash flood simulation using steady-state flow solvers* (EGU22-6953). EGU22. Copernicus Meetings. https://doi.org/10.5194/egusphere-egu22-6953

Bulti, D. T., & Abebe, B. G. (2020). Analyzing the impacts of urbanization on runoff characteristics in Adama city, Ethiopia. *SN Applied Sciences*, *2*(7), 1151. https://doi.org/10.1007/s42452-020-2961-3

Burian, S., & Durrans, S. (2002). Short Time-Interval Rainfall Disaggregation for Continuous Hydrologic Simulation. *Journal of Water Management Modeling*. https://doi.org/10.14796/JWMM.R208-04

Chen, Y.-R., Yeh, C.-H., & Yu, B. (2011). Integrated application of the analytic hierarchy process and the geographic information system for flood risk assessment and flood plain management in Taiwan. *Natural Hazards*, *59*(3), 1261–1276. https://doi.org/10.1007/s11069-011-9831-7

Chow, W. T. L., Cheong, B. D., & Ho, B. H. (2016). A Multimethod Approach towards Assessing Urban Flood Patterns and Its Associated Vulnerabilities in Singapore. *Advances in Meteorology*, *2016*, e7159132. https://doi.org/10.1155/2016/7159132

Desalegn, H., & Mulu, A. (2021). Flood vulnerability assessment using GIS at Fetam watershed, upper Abbay basin, Ethiopia. *Heliyon*, *7*(1), e05865. https://doi.org/10.1016/j.heliyon.2020.e05865

Elkhrachy, I. (2015). Flash Flood Hazard Mapping Using Satellite Images and GIS Tools: A case study of Najran City, Kingdom of Saudi Arabia (KSA). *The Egyptian Journal of Remote Sensing and Space Science*, *18*(2), 261–278. https://doi.org/10.1016/j.ejrs.2015.06.007

Engida, A. N., & Esteves, M. (2011). Characterization and disaggregation of daily rainfall in the Upper Blue Nile Basin in Ethiopia. *Journal of Hydrology*, *399*(3), 226–234. https://doi.org/10.1016/j.jhydrol.2011.01.001

Fikadu, S. (2012). *Flood risk mapping and Vulnerability Analysis*. 64.

Fowler, H. J., Wasko, C., & Prein, A. F. (2021). Intensification of short-duration rainfall extremes and implications for flood risk: Current state of the art and future directions. *Philosophical Transactions. Series A, Mathematical, Physical, and Engineering Sciences*, *379*(2195), 20190541. https://doi.org/10.1098/rsta.2019.0541

Gebre SL, G. Y. (2015). Flood Hazard Assessment and Mapping of Flood Inundation Area of the Awash River Basin in Ethiopia using GIS and HEC-GeoRAS/HEC-RAS Model. *Journal of Civil & Environmental Engineering*, *05*(04). https://doi.org/10.4172/2165-784X.1000179

Gezahegn, M., & Suryabhagavan, K. (2018). *Developing Flood Hazard Forecasting and Early Warning System in Dire Dawa, Ethiopia*. *5*, 11–27. https://doi.org/10.22192/ijamr.2018.05.09.003

Gigović, L., Pamučar, D., Bajić, Z., & Drobnjak, S. (2017). Application of GIS-Interval Rough AHP Methodology for Flood Hazard Mapping in Urban Areas. *Water*, *9*(6), Article 6. https://doi.org/10.3390/w9060360

Guo, S.-Y., Li, L., Zhang, L.-J., Li, Y.-L., Li, S.-Z., & Xu, J. (2021). From the One Health Perspective: Schistosomiasis Japonica and Flooding. *Pathogens*, *10*(12), Article 12. https://doi.org/10.3390/pathogens10121538

Hagos, Y. G., Andualem, T. G., Yibeltal, M., & Mengie, M. A. (2022). Flood hazard assessment and mapping using GIS integrated with multi-criteria decision analysis in upper Awash River basin, Ethiopia. *Applied Water Science*, *12*(7), 148. https://doi.org/10.1007/s13201-022-01674-8

Hategekimana, Y., Yu, L., Nie, Y., Zhu, J., Liu, F., & Guo, F. (2018). Integration of multi-parametric fuzzy analytic hierarchy process and GIS along the UNESCO World Heritage: A flood hazard index, Mombasa County, Kenya. *Natural Hazards*, *92*(2), 1137–1153. https://doi.org/10.1007/s11069-018-3244-9

Hemmati, M., Ellingwood, B. R., & Mahmoud, H. N. (2020). The Role of Urban Growth in Resilience of Communities Under Flood Risk. *Earth's Future*, *8*(3), e2019EF001382. https://doi.org/10.1029/2019EF001382

Iliadis, C., Galiatsatou, P., Glenis, V., Prinos, P., & Kilsby, C. (2023). Urban Flood Modelling under Extreme Rainfall Conditions for Building-Level Flood Exposure Analysis. *Hydrology*, *10*(8), Article 8. https://doi.org/10.3390/hydrology10080172

Jemberie, M. A., & Melesse, A. M. (2021). Urban Flood Management through Urban Land Use Optimization Using LID Techniques, City of Addis Ababa, Ethiopia. *Water*, *13*(13), Article 13. https://doi.org/10.3390/w13131721

Kassegn, A., & Endris, E. (2021). Review on socio-economic impacts of 'Triple Threats' of COVID-19, desert locusts, and floods in East Africa: Evidence from Ethiopia. *Cogent Social Sciences*, *7*(1), 1885122. https://doi.org/10.1080/23311886.2021.1885122

Khajehei, S., Ahmadalipour, A., Shao, W., & Moradkhani, H. (2020). A Place-based Assessment of Flash Flood Hazard and Vulnerability in the Contiguous United States. *Scientific Reports*, *10*(1), Article 1. https://doi.org/10.1038/s41598-019-57349-z

Khalaj, M. R., Noor, H., & Dastranj, A. (2021). Investigation and simulation of flood inundation hazard in urban areas in Iran. *Geoenvironmental Disasters*, *8*(1), 18. https://doi.org/10.1186/s40677-021-00191-1

Koriche, S. A. (2012). *Remote Sensing Based Hydrological Modelling for Flood Early Warning In The Upper And Middle Awash River Basin*. 67.

Koutsoyiannis, D. (2003). *Rainfall disaggregation methods: Theory and applications* (pp. 1–23). https://doi.org/10.13140/RG.2.1.2840.8564

Lane, S. N. (2017). Natural flood management. *WIREs Water*, *4*(3), e1211. https://doi.org/10.1002/wat2.1211

Mahmoud, S. H., & Gan, T. Y. (2018). Multi-criteria approach to develop flood susceptibility maps in arid regions of Middle East. *Journal of Cleaner Production*, *196*, 216–229. https://doi.org/10.1016/j.jclepro.2018.06.047

Maidment, R. I., Grimes, D., Black, E., Tarnavsky, E., Young, M., Greatrex, H., Allan, R. P., Stein, T., Nkonde, E., Senkunda, S., & Alcántara, E. M. U. (2017). A new, long-term daily satellite-based rainfall dataset for operational monitoring in Africa. *Scientific Data*, *4*(1), Article 1. https://doi.org/10.1038/sdata.2017.63

Marco, J. B. (1994). Flood risk mapping. In G. Rossi, N. Harmancioğlu, & V. Yevjevich (Eds.), *Coping with Floods* (pp. 353–373). Springer Netherlands. https://doi.org/10.1007/978-94-011-1098-3_20

Massari, C., Brocca, L., Pellarin, T., Abramowitz, G., Filippucci, P., Ciabatta, L., Maggioni, V., Kerr, Y., & Fernandez Prieto, D. (2020). A daily 25 km short-latency rainfall product for data-scarce regions based on the integration of the Global Precipitation Measurement mission rainfall and multiple-satellite soil moisture products. *Hydrology and Earth System Sciences*, *24*(5), 2687–2710. https://doi.org/10.5194/hess-24-2687-2020

Mehedi, M. A. A., Smith, V., Hosseiny, H., & Jiao, X. (2022). Unraveling the complexities of urban fluvial flood hydraulics through AI. *Scientific Reports, 12*(1), Article 1. https://doi.org/10.1038/s41598-022-23214-9

Morea, H., & Samanta, S. (2020). Multi-criteria decision approach to identify flood vulnerability zones using geospatial technology in the Kemp-Welch Catchment, Central Province, Papua New Guinea. *Applied Geomatics, 12*(4), 427–440. https://doi.org/10.1007/s12518-020-00315-6

Nasiri, H., Mohd Yusof, M. J., & Mohammad Ali, T. A. (2016). An overview to flood vulnerability assessment methods. *Sustainable Water Resources Management*, *2*(3), 331–336. https://doi.org/10.1007/s40899-016-0051-x

Nigusse, A. G., & Adhanom, O. G. (2019). Flood Hazard and Flood Risk Vulnerability Mapping Using Geo-Spatial and MCDA around Adigrat, Tigray Region, Northern Ethiopia. *Momona Ethiopian Journal of Science*, *11*(1), Article 1. https://doi.org/10.4314/mejs.v11i1

OCHA. (2020). *Floods and locust outbreak snapshot*. http://scholar.googleusercontent.com/scholar?q=cache:B18_mhP_0g4J:scholar.google.com/+United+Nations+Office+for+the+Coordination+of+Humanitarian+Affairs+%5BOCHA%5D,+2020aOCHA.+(2020a).+Eastern+Africa+region:+Floods+and+locust+outbreak+snapshot,+May+2020.+https://reliefweb.int/report/ethiopia/eastern-africa-region-floods-and-locust-outbreak-snap&hl=en&as_sdt=0,5

O’Donnell, E. C., & Thorne, C. R. (2020). Drivers of future urban flood risk. *Philosophical Transactions. Series A, Mathematical, Physical, and Engineering Sciences*, *378*(2168), 20190216. https://doi.org/10.1098/rsta.2019.0216

OFDA. (2012). *Annual disaster statistical review: WHO collaborating centre for research on the epidemiology of disasters*. 52.

Ogato, G. S., Bantider, A., Abebe, K., & Geneletti, D. (2020). Geographic information system (GIS)-Based multicriteria analysis of flooding hazard and risk in Ambo Town and its watershed, West shoa zone, oromia regional State, Ethiopia. *Journal of Hydrology: Regional Studies*, *27*, 100659. https://doi.org/10.1016/j.ejrh.2019.100659

Ologunorisa et al. (2005). *+Bioline International Official Site (site up-dated regularly)*. http://www.bioline.org.br/request?ja05010

Ouma, Y. O., & Tateishi, R. (2014). Urban Flood Vulnerability and Risk Mapping Using Integrated Multi-Parametric AHP and GIS: Methodological Overview and Case Study Assessment. *Water*, *6*(6), Article 6. https://doi.org/10.3390/w6061515

Papaioannou, G., Efstratiadis, A., Vasiliades, L., Loukas, A., Papalexiou, S. M., Koukouvinos, A., Tsoukalas, I., & Kossieris, P. (2018). An Operational Method for Flood Directive

Implementation in Ungauged Urban Areas. *Hydrology*, *5*(2), Article 2. https://doi.org/10.3390/hydrology5020024

Phongsapan, K., Chishtie, F., Poortinga, A., Bhandari, B., Meechaiya, C., Kunlamai, T., Aung, K. S., Saah, D., Anderson, E., Markert, K., Markert, A., & Towashiraporn, P. (2019). Operational Flood Risk Index Mapping for Disaster Risk Reduction Using Earth Observations and Cloud Computing Technologies: A Case Study on Myanmar. *Frontiers in Environmental Science*, *7*. https://www.frontiersin.org/articles/10.3389/fenvs.2019.00191

Rimba, A. B., Setiawati, M. D., Sambah, A. B., & Miura, F. (2017). Physical Flood Vulnerability Mapping Applying Geospatial Techniques in Okazaki City, Aichi Prefecture, Japan. *Urban Science*, *1*(1), Article 1. https://doi.org/10.3390/urbansci1010007

Rincón, D., Khan, U. T., & Armenakis, C. (2018). Flood Risk Mapping Using GIS and Multi-Criteria Analysis: A Greater Toronto Area Case Study. *Geosciences*, *8*(8), Article 8. https://doi.org/10.3390/geosciences8080275

Rubinato, M., Nichols, A., Peng, Y., Zhang, J., Lashford, C., Cai, Y., Lin, P., & Tait, S. (2019). Urban and river flooding: Comparison of flood risk management approaches in the UK and China and an assessment of future knowledge needs. *Water Science and Engineering*, *12*(4), 274–283. https://doi.org/10.1016/j.wse.2019.12.004

Saaty, T. L. (1980). *Fundamentals of Decision Making and Priority Theory with the Analytic Hierarchy Process*. RWS Publications.

Saaty, T. L. (1987). Risk-Its Priority and Probability: The Analytic Hierarchy Process. *Risk Analysis*, *7*(2), 159–172. https://doi.org/10.1111/j.1539-6924.1987.tb00980.x

Saaty, T. L. (2008). Decision making with the analytic hierarchy process. *International Journal of Services Sciences*, *1*(1), 83. https://doi.org/10.1504/IJSSCI.2008.017590

Samuels, P. G. (2006). A European Perspective on Current Challenges in The Analysis of Inland Flood Risks. In J. Schanze, E. Zeman, & J. Marsalek (Eds.), *Flood Risk Management: Hazards, Vulnerability and Mitigation Measures* (pp. 21–34). Springer Netherlands. https://doi.org/10.1007/978-1-4020-4598-1_2

Saxton, K. E., & Rawls, W. J. (2006). Soil Water Characteristic Estimates by Texture and Organic Matter for Hydrologic Solutions. *Soil Science Society of America Journal*, *70*(5), 1569–1578. https://doi.org/10.2136/sssaj2005.0117

Schoenherr, T., Rao Tummala, V. M., & Harrison, T. P. (2008). Assessing supply chain risks with the analytic hierarchy process: Providing decision support for the offshoring decision by a US manufacturing company. *Journal of Purchasing and Supply Management*, *14*(2), 100–111. https://doi.org/10.1016/j.pursup.2008.01.008

Singh, P., Sinha, V. S. P., Vijhani, A., & Pahuja, N. (2018). Vulnerability assessment of urban road network from urban flood. *International Journal of Disaster Risk Reduction*, *28*, 237–250. https://doi.org/10.1016/j.ijdrr.2018.03.017

Sulaiman, N. A., Husain, F., Hashim, K. A., & Samad, Abd. M. (2012). A study on flood risk assessment for Bandar Segamat sustainability using remote sensing and GIS approach. *2012 IEEE Control and System Graduate Research Colloquium*, 386–391. https://doi.org/10.1109/ICSGRC.2012.6287197

Sun, X., Li, R., Shan, X., Xu, H., & Wang, J. (2021). Assessment of climate change impacts and urban flood management schemes in central Shanghai. *International Journal of Disaster Risk Reduction*, *65*, 102563. https://doi.org/10.1016/j.ijdrr.2021.102563

Tanoue, M., Hirabayashi, Y., & Ikeuchi, H. (2016). Global-scale river flood vulnerability in the last 50 years. *Scientific Reports*, *6*(1), Article 1. https://doi.org/10.1038/srep36021

Tesema, D. (2017). *Assessment of Adama City Flood Risk Using Multicriteria Approach*. *IV*, 6–24.

USGS. (2003). *Effects of Urban Development on Floods*. https://pubs.usgs.gov/fs/fs07603/

van den Bout, B., Jetten, V. G., van Westen, C. J., & Lombardo, L. (2023). A breakthrough in fast flood simulation. *Environmental Modelling & Software*, 105787. https://doi.org/10.1016/j.envsoft.2023.105787

Wang, J.-J., & Yang, D.-L. (2007). Using a hybrid multi-criteria decision aid method for information systems outsourcing. *Computers & Operations Research*, *34*(12), 3691–3700. https://doi.org/10.1016/j.cor.2006.01.017

Wang, Z., Lai, C., Chen, X., Yang, B., Zhao, S., & Bai, X. (2015). Flood hazard risk assessment model based on random forest. *Journal of Hydrology*, *527*, 1130–1141. https://doi.org/10.1016/j.jhydrol.2015.06.008

Weldegebriel, Z. B., & Amphune, B. E. (2017). Livelihood resilience in the face of recurring floods: An empirical evidence from Northwest Ethiopia. *Geoenvironmental Disasters*, *4*(1), 10. https://doi.org/10.1186/s40677-017-0074-0

WMO. (2021). *Water-related hazards dominate disasters in the past 50 years*. http://119.78.100.173/C666//handle/2XK7JSWQ/332820

Wondim, Y. K. (2016). *Flood Hazard and Risk Assessment Using GIS and Remote Sensing in Lower Awash Sub-basin, Ethiopia*. *VI* (2225–0948), 19.

Yazdi, J., Yoo, D. G., & Kim, J. H. (2017). Comparative study of multi-objective evolutionary algorithms for hydraulic rehabilitation of urban drainage networks. *Urban Water Journal*, *14*(5), 483–492. https://doi.org/10.1080/1573062X.2016.1223319

Yeganeh, N., & Sabri, S. (2014). Flood Vulnerability Assessment in Iskandar Malaysia Using Multi-Criteria Evaluation and Fuzzy Logic. *Research Journal of Applied Sciences, Engineering and Technology*, *8*, 1794–1806. https://doi.org/10.19026/rjaset.8.1167

Zhao, H., Gu, T., Tang, J., Gong, Z., & Zhao, P. (2023). Urban flood risk differentiation under land use scenario simulation. *IScience*, *26*(4), 106479. https://doi.org/10.1016/j.isci.2023.106479

APPENDICES

Appendix Table 1. normalized pair-wise comparison matrix computation

Factors	Elevation	DD	LULC	Road network	Slope	Storm drains	RF	Soil type	SUM	CW	%CW
Elevation	0.253	0.248	0.329	0.252	0.166	0.216	0.171	0.186	1.821	0.228	22.762
DD	0.253	0.248	0.329	0.252	0.166	0.172	0.171	0.155	1.747	0.218	21.837
LULC	0.084	0.083	0.110	0.189	0.249	0.172	0.086	0.155	1.128	0.141	14.098
Road network	0.063	0.062	0.037	0.063	0.249	0.129	0.029	0.155	0.787	0.098	9.834
Slope	0.127	0.124	0.037	0.021	0.083	0.129	0.171	0.155	0.847	0.106	10.583
Storm drains	0.051	0.062	0.027	0.021	0.028	0.043	0.029	0.155	0.415	0.052	5.188
RF	0.127	0.124	0.110	0.189	0.042	0.129	0.086	0.010	0.816	0.102	10.202
Soil type	0.042	0.050	0.022	0.013	0.017	0.009	0.257	0.031	0.440	0.055	5.495

Appendix Table 2. consistency of pair-wise matrix

Factors	Elevation	DD	LULC	RN	Slope	Storm drains	RF	Soil type	WSV	CW	WSV/WC
Elevation	0.228	0.218	0.423	0.393	0.212	0.259	0.204	0.330	2.267	0.228	9.960
DD	0.228	0.218	0.423	0.393	0.212	0.208	0.204	0.275	2.160	0.218	9.893
LULC	0.076	0.073	0.141	0.295	0.317	0.208	0.102	0.275	1.486	0.141	10.543
Road network	0.057	0.055	0.047	0.098	0.317	0.156	0.034	0.275	1.039	0.098	10.563
Slope	0.114	0.109	0.047	0.033	0.106	0.156	0.204	0.275	1.043	0.106	9.856
Storm drains	0.046	0.055	0.035	0.033	0.035	0.052	0.034	0.275	0.564	0.052	10.872
RF	0.114	0.109	0.141	0.295	0.053	0.156	0.102	0.018	0.988	0.102	9.683
Soil type	0.038	0.044	0.028	0.020	0.021	0.010	0.306	0.055	0.522	0.055	9.500
										Lmax	10.1

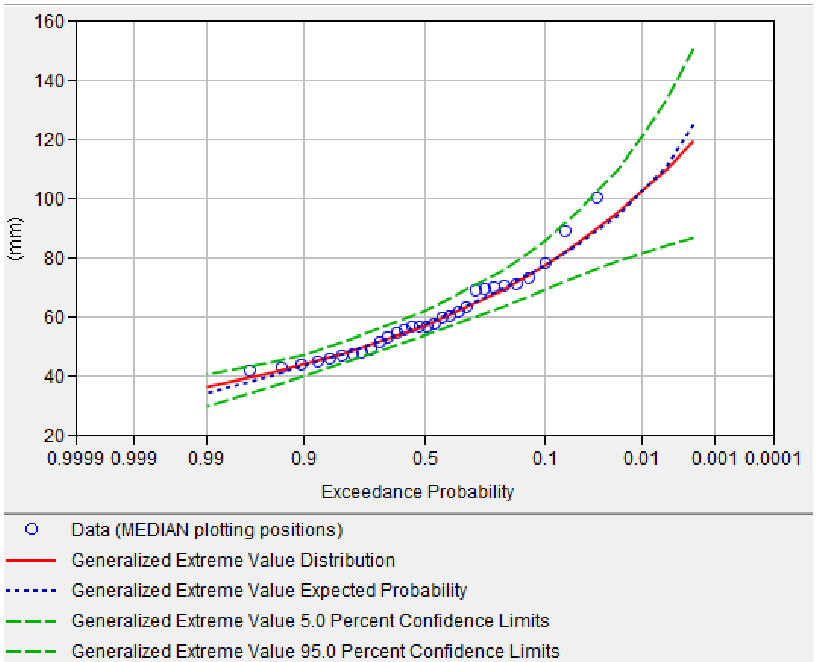

Appendix Figure 1. distribution fitness test using Kolmogorov-Smirnov statistics test

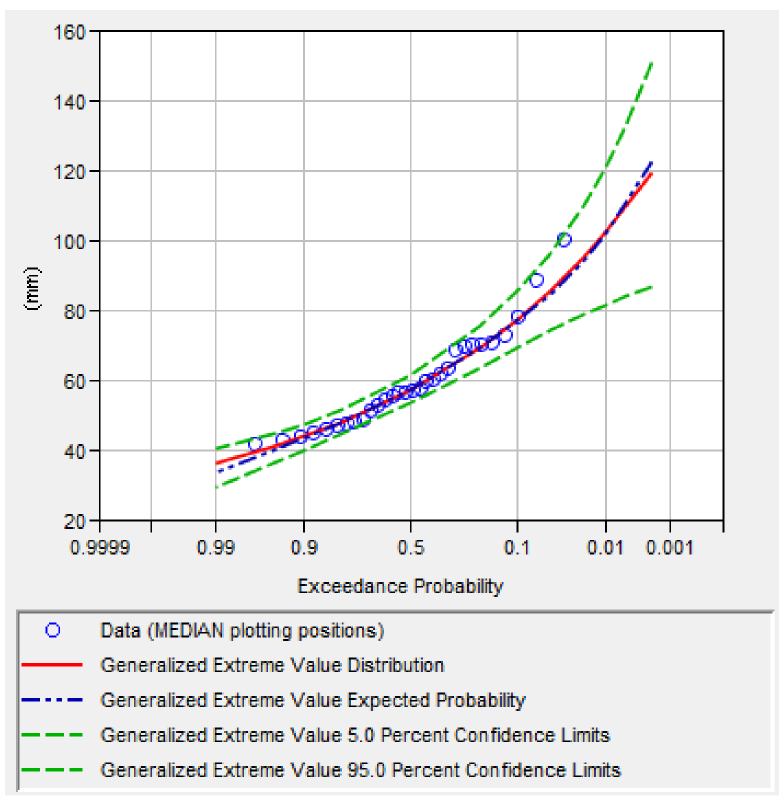

Appendix Figure 2. distribution fitness test using chi-square statistics test

Select Distribution Types to Display

Filter Distributions | Filter Goodness of Fit

Standard Product Moments | L- Moments

Distributions	Kolmogorov-Smirnov (Test Statistic)	Chi-Square (Test Statistic)
Generalized Extreme Value	0.087	0.800
Generalized Pareto	0.087	2.800
Gumbel	0.088	0.800
Ln-Normal	0.089	1.200
Log10-Normal	0.089	1.200
Normal	0.127	1.600
Logistic	0.135	0.800
Exponential	0.504	74.400
Empirical	N/A	N/A
Generalized Logistic	NaN	NaN

Appendix Figure 3. Kolmogorov-Smirnov and chi-square statistics test

Appendix Figure 4. pictures of closed storm drains by dirt’s, solid wastes and soil

Title: Survey on Relative Importance Weights of Flood Causative Factors in Adama City, Ethiopia

Objective: Application of Integrated Multi-Parametric AHP-GIS for Flood Vulnerability and Risk Mapping

Please put your name, organization and field of study in the space provided.

1. Name: ______________________________
2. Affiliation/Organization: ______________________
3. Expertise/Field of study: ______________________

Instructions: Please compare each flood causative factor with each other as tabulated in table 2 by selecting either A or B under relative importance column and assign a weight on a scale of 1 to 9 under the column of rank.

Table1: Nine-point intensity of importance scale

Scale	Definition	Description
1	Equally important	Two factors contribute equally to the objective.
3	Moderately more important	Experience and judgment slightly favor one over the other
5	Strongly more important	Experience and judgment strongly favor one over the other
7	Very strong more important	Experience and judgment very strongly favor one over the other, its importance is demonstrated in practice
9	Extremely more important	The evidence favoring one over the other is of the highest possible validity
2,4,6,8	Intermediate values	When compromise is needed or to express intermediate values

Note1: Reciprocal of the above scale (1-9) is filled for element compared with the assigned one

Note2: Refer table 1 to fill table 2.

QUESTIONNAIRE PROVIDED FOR FLOOD VULNERABLITY AND RISK MAPPING OF ADAMA CITY, ETH.

Table2: Relative Importance Weights of Flood Causative Factors in Adama City

CRITERIAS		Relative Importance	Rank
A	B	A/B	scale (1 to 9)
Elevation	Drainage density		
	LULC		
	Road network		
	Slope		
	Storm drain		
	Rainfall		
	Soil type		
Drainage density	LULC		
	Road network		
	Slope		
	Storm drain		
	Rainfall		
	Soil type		
LULC	Road network		
	Slope		
	Storm drain		
	Rainfall		
	Soil type		
Road network	Slope		
	Storm drain		
	Rainfall		
	Soil type		
Slope	Storm drain		
	Rainfall		
	Soil type		
Storm drain	Rainfall		
	Soil type		
Soil type	Soil type		

Optional comment: Please provide additional comment regarding the relative importance weights of flood causative factors in Adama city.

Appendix figure 5. Questionnaire papers